The Astrophysical Journal, 624:638–655, 2005 May 10

A SURVEY OF UNIDENTIFIED EGRET SOURCES AT VERY HIGH ENERGIES

S. J. Fegan,[1,2,3] H. M. Badran,[4] I. H. Bond,[5] P. J. Boyle,[6] S. M. Bradbury,[5] J. H. Buckley,[7] D. A. Carter-Lewis,[8] M. Catanese,[1] O. Celik,[9] W. Cui,[10] M. Daniel,[8] M. D'Vali,[5] I. de la Calle Perez,[11] C. Duke,[12] A. Falcone,[10] D. J. Fegan,[13] J. P. Finley,[10] L. F. Fortson,[14,15] J. A. Gaidos,[10] S. Gammell,[13] K. Gibbs,[1] G. H. Gillanders,[16] J. Grube,[5] J. Hall,[17] T. A. Hall,[18] D. Hanna,[19] A. M. Hillas,[5] J. Holder,[5] D. Horan,[1] A. Jarvis,[9] M. Jordan,[7] G. E. Kenny,[16] M. Kertzman,[20] D. Kieda,[17] J. Kildea,[19] J. Knapp,[5] K. Kosack,[7] H. Krawczynski,[7] F. Krennrich,[8] M. J. Lang,[16] S. Le Bohec,[8] R. W. Lessard,[10] E. Linton,[6] J. Lloyd-Evans,[5] A. Milovanovic,[5] J. McEnery,[21] P. Moriarty,[22] R. Mukherjee,[23] D. Muller,[6] T. Nagai,[17] S. Nolan,[10] R. A. Ong,[9] R. Pallassini,[5] D. Petry,[22] B. Power-Mooney,[13] J. Quinn,[13] M. Quinn,[13] K. Ragan,[19] P. Rebillot,[7] P. T. Reynolds,[24] H. J. Rose,[5] M. Schroedter,[1,2] G. H. Sembroski,[10] S. P. Swordy,[6] A. Syson,[5] V. V. Vassiliev,[9] S. P. Wakely,[6] G. Walker,[17] T. C. Weekes,[1] and J. Zweerink[9]

Received 2004 October 4; accepted 2005 January 22

ABSTRACT

The Whipple Observatory 10 m γ-ray telescope has been used to survey the error boxes of EGRET unidentified sources in an attempt to find counterparts at energies of 350 GeV and above. Twenty-one unidentified sources detected by EGRET (more than 10% of the total number) have been included in this survey. In no case is a statistically significant signal found in the EGRET error box, which implies that, at least for this sample, the γ-ray spectra of these sources steepen between 100 MeV and 350 GeV. For each EGRET source location, we list candidate associations and derive upper limits on the integral γ-ray flux above 350 GeV.

Subject headings: galaxies: jets — gamma rays: observations — surveys

Online material: color figures

1. INTRODUCTION

The number of confirmed sources of γ-ray emission at very high energies ($E > 100$ GeV) is still small (Horan & Weekes 2004), but the number is increasing as the sensitivity of ground-based γ-ray observatories improves. All of the source discoveries to date have come from observations using the atmospheric Cerenkov imaging technique. In these observations the telescopes, which typically have fields of view of less than 5°, have been directed at sources that observations at longer wavelengths have suggested as potential TeV sources. Several of the TeV sources show evidence of the Compton-synchrotron mechanism; hence a fruitful predictor of TeV emission comes from observations in hard X-rays. In principle, sources that are known to emit MeV and GeV γ-rays, i.e., those from the Third EGRET Catalog (Hartman et al. 1999) and from the GeV catalog compiled from the same database (Lamb & Macomb 1997), should also be strong candidates for TeV emission, particularly since many of the sources exhibit power-law spectra with hard spectral indices. In practice, although the (νF_ν) sensitivities of the ground-based TeV telescopes and the space-based MeV/GeV telescopes are similar, less than half of the detected TeV sources were seen by EGRET, indicating that the population of sources emitting in the MeV–GeV and TeV bands are quasi-independent. Nevertheless the EGRET source catalogs are fruitful starting points for TeV γ-ray source searches.

One of the significant legacies of the EGRET mission on the *Compton Gamma Ray Observatory* was the large number of detected sources for which no obvious counterpart was found at longer wavelengths and whose nature therefore remains elusive (Hartman et al. 1999; Lamb & Macomb 1997; Macomb & Lamb 1999). The lack of identification is not surprising since the EGRET error boxes are typically of 1° diameter and the number of candidate objects very large. Hartman et al. (1999) list identifications for approximately 80 of the EGRET sources, with

[1] Fred Lawrence Whipple Observatory, Harvard-Smithsonian CfA, P.O. Box 97, Amado, AZ 85645-0097; sfegan@astro.ucla.edu.
[2] Department of Physics, University of Arizona, Tucson, AZ 85721.
[3] Current address: Department of Physics, University of California, Los Angeles, CA 90095-1562.
[4] Physics Department, Tanta University, Tanta, Egypt.
[5] Department of Physics, University of Leeds, Leeds LS2 9JT, West Yorkshire, UK.
[6] Enrico Fermi Institute, University of Chicago, Chicago, IL 60637.
[7] Department of Physics, Washington University, St. Louis, MO 63130.
[8] Department of Physics and Astronomy, Iowa State University, Ames, IA 50011-3160.
[9] Department of Physics, University of California, Los Angeles, CA 90095-1562.
[10] Department of Physics, Purdue University, West Lafayette, IN 47907.
[11] University of Oxford, Physics Department, Denys Wilkinson Building, Keble Road, Oxford OX1 3RH, UK.
[12] Department of Physics, Grinnell College, Grinnell, IA 50112-1690.
[13] Experimental Physics Department, National University of Ireland, Belfield, Dublin 4, Ireland.
[14] Department of Astronomy and Astrophysics, University of Chicago, Chicago, IL.
[15] Astronomy Department, Adler Planetarium and Astronomy Museum, Chicago, IL.
[16] Department of Physics, National University of Ireland, Galway, Ireland.
[17] High Energy Astrophysics Institute, University of Utah, Salt Lake City, UT 84112.
[18] Department of Physics and Astronomy, University of Arkansas, Little Rock, AR 72204-1099.
[19] Physics Department, McGill University, Montreal, QC H3A 2T8, Canada.
[20] Department of Physics and Astronomy, DePauw University, Greencastle, IN 46135-0037.
[21] School of Science, Galway-Mayo Institute of Technology, Galway, Ireland.
[22] University of Maryland, Baltimore County and NASA/GSFC.
[23] Department of Physics and Astronomy, Barnard College, New York, NY 10027.
[24] Department of Applied Physics and Instrumentation, Cork Institute of Technology, Cork, Ireland.

TABLE 1

COMPARISON OF THE CHARACTERISTICS OF THE EGRET INSTRUMENT ON CGRO AND THE WHIPPLE 10 m ATMOSPHERIC CERENKOV IMAGING TELESCOPE

Characteristic	EGRET	Whipple
Energy range (MeV)	30 to 3×10^4	3×10^5 to 3×10^7
Effective area (cm^2)	1200 at 100 MeV	2×10^8 at 350 GeV
	1600 at 500 MeV	4.4×10^8 at 1 TeV
	1400 at 3000 MeV	3.6×10^8 at 10 TeV
Average error in γ-ray origin (θ_{68}) (deg)	5.85 at 100 MeV	...
	1.71 at 1 GeV	0.42 at 300 GeV
	0.50 at 10 GeV	0.25 at 1 TeV
Field of view (sr)	~0.6	0.0012
Sensitivity to Crab Nebula–like spectrum (cm^{-2} s^{-1})	6×10^{-8} > 100 MeV ($3\ \sigma$ after 2 weeks off Galactic plane)	3.02×10^{-11} > 350 GeV or 0.294 × Crab flux ($4\ \sigma$ in 5 hr)

known active galactic nuclei (AGNs) and pulsars. The remainder of the sources were not firmly identified. Extensive studies have been made at radio, optical, and X-ray wavelengths to find objects that can be identified as counterparts (e.g., Halpern et al. 2001b), and there are a number of promising possibilities. In total, one could now consider approximately 130 of the EGRET sources as having identifications (e.g., Sowards-Emmerd et al. 2003; Mattox et al. 2001). However, a new and distinct class of object has not emerged and the nature of the remaining 140 unidentified sources is still a subject of speculation. Another approach has been to associate the distribution of subsets of the sources with the distribution of known classes of objects (e.g., Roberts et al. 2001; Gehrels et al. 2000), but such associations are ambiguous and this approach does not reveal individual identifications.

Atmospheric Cerenkov imaging telescopes are ideally suited to the study of unidentified EGRET sources since the fields of view of typical Cerenkov cameras are considerably larger than the EGRET error boxes. Although these telescopes have optimum sensitivity for sources in the center of the field of view, i.e., on the optical axis, sensitive search techniques have been developed to search for sources that are not on the axis (Akerlof et al. 1991; Lessard et al. 2001). For the Whipple Telescope, the flux sensitivity at $1^\circ.0$ off axis is ~50% of that on axis (Fegan et al. 2001). The telescope has been shown to have flux sensitivity even outside the geometrical field of view of the camera. The relative sensitivity of the Whipple Telescope, with the camera used in this survey, is contrasted with the EGRET instrument in Table 1.

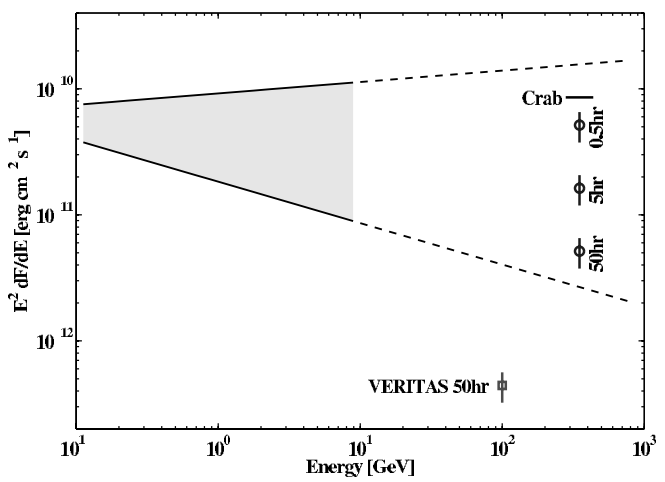

FIG. 1.—Comparison of upper limit on source luminosity derivable through observations at Whipple with the extrapolated luminosity of a "mean" 100 MeV source. Upper limits for 0.5, 5, and 50 hr observations are shown, assuming a Crab Nebula–like spectrum. The hypothetical 100 MeV source has an integral flux spectrum given by the mean flux and spectral index from 3EG sources chosen for this survey: $I(>E) = (30.9 \pm 4.1) \times 10^{-8}(E/100\ \mathrm{MeV})^{-1.12 \pm 0.21}\ \mathrm{cm}^{-2}\ \mathrm{s}^{-1}$. The upper limits are derived by assuming that the VHE emission is from a source with a spectral index similar to that of the Crab Nebula in this energy regime, i.e., $\Gamma \approx 2.5$. The point marked as "VERITAS 50 hr" indicates the limits that can be derived from 50 hr of observations with a ground-based array such as VERITAS-4 or HESS. [*See the electronic edition of the Journal for a color version of this figure.*]

The Whipple instrument has a detection sensitivity of ≈30% of the flux of the Crab in 5 hr of observation (for a detection at the $4\ \sigma$ level). The potential of such ground-based observations is illustrated in Figure 1, where the upper limit that can be placed on the source flux above 350 GeV from observations with various durations is shown relative to a hypothetical EGRET source. The spectrum of this hypothetical source is, in fact, the mean of the sources in the EGRET catalog that were used in this survey: $I(>E) = (30.9 \pm 4.1) \times 10^{-8}(E/100\ \mathrm{MeV})^{-1.12 \pm 0.21}\ \mathrm{cm}^{-2}\ \mathrm{s}^{-1}$. The upper limits are derived by assuming that the very high energy (VHE) emission is from a source with a spectral index similar to that of the Crab Nebula in the VHE regime, i.e., $\Gamma \approx 2.5$.

Previous studies with an earlier version of the Whipple TeV γ-ray telescope have been reported (Buckley et al. 1997) on a limited number of unidentified EGRET sources. The HEGRA group has reported observations on five sources from the GeV catalog with sensitive upper limits, 1%–10% of the Crab (Rowell et al. 2003). This paper reports the results of a survey of 21 unidentified EGRET source fields (more than 10% of the total number of unidentified EGRET sources).

2. SOURCE LIST

It is not possible to isolate the subclasses of unidentified source from the EGRET and GeV catalogs that would be the best candidates for VHE γ-ray emission. In principle the strongest sources with the hardest spectra should be included in a survey. However, the spectra, particularly those of the weaker sources, are not well determined, and extrapolation of power-law spectra to detectable levels at very high energies is a distinct possibility. In practice operational considerations played a major role in the selection of survey sources. These considerations included

1. choice of declination so that the source transited within 30° of the zenith to give maximum sensitivity;
2. sources that lie at right ascensions that are not well populated with known TeV sources and do not transit during the Arizona monsoon season; and

TABLE 2

Summary of the 3EG and GeV Catalog Entries for the 19 Unidentified Sources Selected for Observation in the Survey

No.	Source Name	Coordinates[a]		Third EGRET Catalog			GeV Catalog		Variability Indexes[b]	
					Spectrum					
		b (deg)	l (deg)	Error θ_{95}[c] (deg)	$F \pm \Delta F$[d]	$\Gamma \pm \Delta\Gamma$[e]	Error θ_{95} (deg)	Flux $F \pm \Delta F$[d]	δ	$\delta_{\rm min}$
1.....	3EG J0010+7309	10.56	119.87	0.25×0.22	42.3 ± 5.5	1.85 ± 0.10	0.43	5.8 ± 1.2	0.26	0
2.....	3EG J0241+6103	0.99	135.85	0.21×0.15	69.3 ± 6.1	2.21 ± 0.07	0.31	6.9 ± 1.3	0.38	0.17
3.....	3EG J0423+1707	−22.21	178.68	0.88×0.65	15.8 ± 2.7	2.43 ± 0.21	...	...	0.42	0
4.....	GeV J0433+2907	−12.58	170.50	0.19×0.16	22.0 ± 2.8	1.90 ± 0.10	0.35	3.3 ± 0.7	0.40	0.10
5.....	3EG J0450+1105	−20.55	187.89	0.65×0.61	14.9 ± 2.5	2.27 ± 0.16	...	...[f]	1.13	0.78
6.....	GeV J0508+0540	−19.81	195.32	...	...	...	0.62	1.4 ± 0.4[g]	...[h]	...[h]
7.....	3EG J0613+4201	11.45	171.38	0.66×0.46	9.0 ± 2.3	1.92 ± 0.26	0.65	1.8 ± 0.6[g]	0.72	0.09
8.....	3EG J0628+1847	3.64	193.60	0.66×0.49	23.9 ± 4.0	2.30 ± 0.10	...	...	...[i]	...[i]
9.....	3EG J0634+0521	−1.22	206.15	0.85×0.50	15.0 ± 3.5	2.03 ± 0.26	...	...[f]	0	0
10.....	3EG J1009+4855	52.15	166.93	1.12×0.80	4.8 ± 1.4	1.90 ± 0.37	...	...	0	0
11.....	3EG J1323+2200	81.15	359.63	0.52×0.43	5.2 ± 1.6	1.86 ± 0.35	...	...[f]	1.09	0.52
12.....	3EG J1337+5029	65.06	105.18	0.77×0.66	9.2 ± 2.6	1.83 ± 0.29	...	...	0.53	0
13.....	3EG J1826−1302	−0.42	18.41	0.55×0.39	46.3 ± 7.3	2.00 ± 0.11	0.32	9.9 ± 1.7	0.88	0.50
14.....	3EG J1835+5918	25.08	88.74	0.16×0.13	60.6 ± 4.4	1.69 ± 0.07	0.27	10.2 ± 1.4	0.15	0
15.....	GeV J1907+0557	−0.88	40.08	...	...	...	0.38×0.28	9.2 ± 1.9	...[h]	...[h]
16.....	GeV J2020+3658	0.24	75.29	0.35×0.26	59.1 ± 6.2	1.86 ± 0.10	0.28×0.21	11.2 ± 1.5	0.36	0.03
17.....	3EG J2227+6122	3.19	106.55	0.50×0.41	41.3 ± 6.1	2.24 ± 0.14	0.54	3.9 ± 1.2[g]	0.20	0
18.....	3EG J2248+1745	−36.15	86.00	1.14×0.78	12.9 ± 3.5	2.11 ± 0.39	...	...	0.65	0
19.....	3EG J2255+1943	−34.35	89.85	2.67×2.33	5.8 ± 2.8	2.36 ± 0.61	...	...	1.18	0.25

[a] Galactic coordinates from the 3EG or GeV catalog as appropriate.
[b] Variability index from Nolan et al. (2003), higher values indicate more source variability.
[c] Elliptical fits to 95% error contours for 3EG sources from Mattox et al. (2001).
[d] Flux and statistical error ($F \pm \Delta F$) at energies greater than 100 MeV in 3EG catalog and 1 GeV in GeV catalog, in units of 10^{-8} cm^{-2} s^{-1}.
[e] Spectral index and error ($\Gamma \pm \Delta\Gamma$) from EGRET catalog (Hartman et al. 1999).
[f] Listed as source of repeating weak outbursts of GeV γ-rays (Table 2 of Macomb and Lamb 1999).
[g] Listed as a low-significance source of GeV γ-rays (Table 2 or 3 of Lamb and Macomb 1997).
[h] Nolan et al. (2003) present variability indices for 3EG sources only.
[i] As noted in Nolan et al. (2003), 3EG J0628+1847 failed a consistency check during the analysis.

3. serendipitous inclusion of an EGRET unidentified source in the ON or OFF fields used in regular Whipple observations.

As a result, the source list surveyed includes 19 sources that appear in both the EGRET and GeV catalogs; their cataloged properties are summarized in Table 2, and their position in the sky relative to the Galactic equator is shown in Figure 2.

3. TECHNIQUE

Cosmic γ-rays at energies greater than 300 GeV are detected at ground level by the Cerenkov radiation given off by the atmosphere caused by the passage of the electromagnetic cascade. The Cerenkov images from the γ-ray–initiated cascades from a point source can be distinguished from the more numerous images resulting from the cascades initiated by charged hadrons in the cosmic radiation by the shape and orientation of the images. The images are recorded in fast cameras made of arrays of photomultipliers in the focal plane of large optical reflectors. The γ-ray observations reported here were made with the GRANITE-III camera (Finley et al. 1999) on the Whipple Observatory 10 m aperture optical reflector (Cawley et al. 1990), which is located on the 2.3 km level of Mount Hopkins in southern Arizona. This is a mature camera-telescope configuration that has been in regular use since 1999; a number of important detections have been reported (Horan et al. 2002; Krennrich et al. 2002; Holder et al. 2003; Kosack et al. 2004).

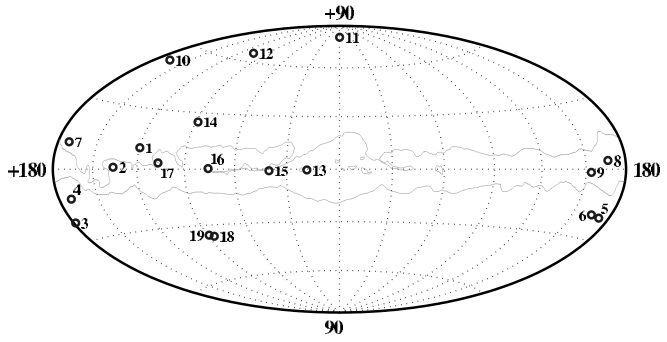

Fig. 2.—The 19 unidentified EGRET sources considered in this survey, plotted in Galactic coordinates and labeled by their positions in Table 2. The outline of the Milky Way, from optical observations (see J. R. Vieira at http://www.skymap.com/milkyway_cat.htm) is depicted for comparison.

4. OBSERVATIONS

Data for this survey were taken from 1999 to 2003 as part of the routine observing program of the Whipple Observatory. Significant changes were made to the telescope during the summer and fall of 2001 when a new technique was applied to the alignment of mirror facets. This bias alignment corrected for the gravitational deformations in the optical support structure with elevation (Schroedter et al. 2002), which is particularly important because of the high resolution of the camera.

Observations with the instrument are made in one of two modes, termed ON/OFF and Tracking modes, which have significantly different approaches to background estimation. When

TABLE 3
OBSERVATION SUMMARY

Source	Epoch of Observations	Duration (minutes)	Observation Mode	Mean Elevation (deg)
3EG J0010+7309	1999–2000	195	ON/OFF	48
3EG J0241+6103	2000–2001	524	ON/OFF	58
3EG J0423+1707	2000–2001	193	ON/OFF	71
GeV J0433+2907	1999–2000	500	ON/OFF	71
	1999–2002	1900	Tracking	75
3EG J0450+1105	2000–2001	264	ON/OFF	68
GeV J0508+0540	2001–2002	842	Tracking	62
3EG J0613+4201	2001–2003	275	ON/OFF	69
3EG J0628+1847	2001–2003	331	ON/OFF	68
3EG J0634+0521	2000–2002	248	ON/OFF	62
3EG J1009+4855	2001–2002	248	ON/OFF	72
3EG J1323+2200	2000–2001	276	ON/OFF	66
3EG J1337+5029	2001–2002	166	ON/OFF	67
3EG J1826–1302	1999–2000	416	ON/OFF	42
3EG J1835+5918	2000–2001	110	ON/OFF	57
GeV J1907+0557	1999–2000	277	ON/OFF	61
GeV J2020+3658	1999–2000	233	ON/OFF	62
3EG J2227+6122	2000–2001	360	ON/OFF	56
3EG J2248+1745	2001–2002	304	ON/OFF	70
3EG J2255+1943	2001–2003	250	ON/OFF	71

operating in the ON/OFF mode, two separate 28 minute scans (ON and OFF) are made. The ON scan is taken while tracking the sky with the candidate object at the center of the field of view and gives an estimate of the γ-ray flux combined with the background rate. The OFF scan is taken in the absence of the candidate object to give an independent estimate of the background rate. The ON and OFF scans are taken such that they are separated by 30 minutes in time and track locations in the sky separated by 30 minutes in right ascension. When operating in the Tracking mode, a single scan is taken tracking the candidate object. An estimate of the background is inferred from the number of events present in the scan that are not consistent with having originated from the candidate source location. The ON/OFF mode can be used to test the hypothesis that the γ-ray emission is occurring from any location within the field of view of the instrument. This is the case for a candidate source whose location is not known a priori, such as unidentified sources with large error-box locations and for sources whose emission is expected to be extended, such as supernova remnants (SNRs). Hence the bulk of the observations taken in this survey were made in the ON/OFF mode.

Table 3 gives a summary of the observations.

5. ANALYSIS

The power of the atmospheric Cerenkov imaging technique depends on the data analysis algorithms that are used to separate candidate γ-ray images from the background of images from cosmic-ray–initiated air showers, local muons, and night-sky noise fluctuations. In general, these algorithms are based on Monte Carlo simulations and optimized using a standard candle such as the Crab Nebula. A number of data analysis algorithms have been developed, for example, *supercuts* developed for data taken at the Whipple 10 m telescope (Punch et al. 1992). This technique typically keeps 50% of γ-ray events and discards >99% of background events. This point-source analysis technique has been adapted to sources whose location is not well defined and to extended sources (Akerlof et al. 1991; Lessard et al. 2001).

Before parameterization, the images are subjected to a series of conditioning routines to ensure that they maintain the maximum information content. The data conditioning steps are routinely applied to all data taken with the Whipple instrument and are described elsewhere (e.g., Lessard et al. 2001). After conditioning, the moments of the light distribution in each image are calculated. From these moments a number of useful parameters are calculated (Reynolds et al. 1993). In particular, the alpha parameter (α) is important to the analysis of data from a candidate point-source object at the center of the field of view. Images with a small value of alpha (usually $\alpha < 15^\circ$) are considered to be consistent with having originated from the source location; those with a large value of alpha are not. In a standard point-source analysis, a histogram is made of the alpha parameter for all events that pass the data selection criteria. An excess of events with small alpha is indicative of a source at the center of the field of view.

For extended sources or sources where the source location is not well determined, it is essential to reconstruct the arrival direction of the primary. For a single telescope, the arrival direction must be inferred from the *shape* and *orientation* of the single observed image. The approach taken here is based on that used in Lessard et al. (2001), with the important difference that a Gaussian smoothing process is applied. The sky map is produced by generating a two-dimensional histogram of the reconstructed arrival directions with respect to the center of the camera. Errors in reconstructing both the image axis and point along the axis from which the γ-ray originated are accounted for by convolving the final two-dimensional map with a Gaussian smoothing function.

Calibration of the two-dimensional analysis method was done using sets of observations of the Crab Nebula, in which the location of the source was deliberately offset from the center of the field of view by various degrees. Calculating the relative γ-ray rate allows a model of the detector response for off-axis and extended sources to be made.

Figure 3 shows significance maps for the Crab Nebula offset by three different amounts. In each of them the Crab source is

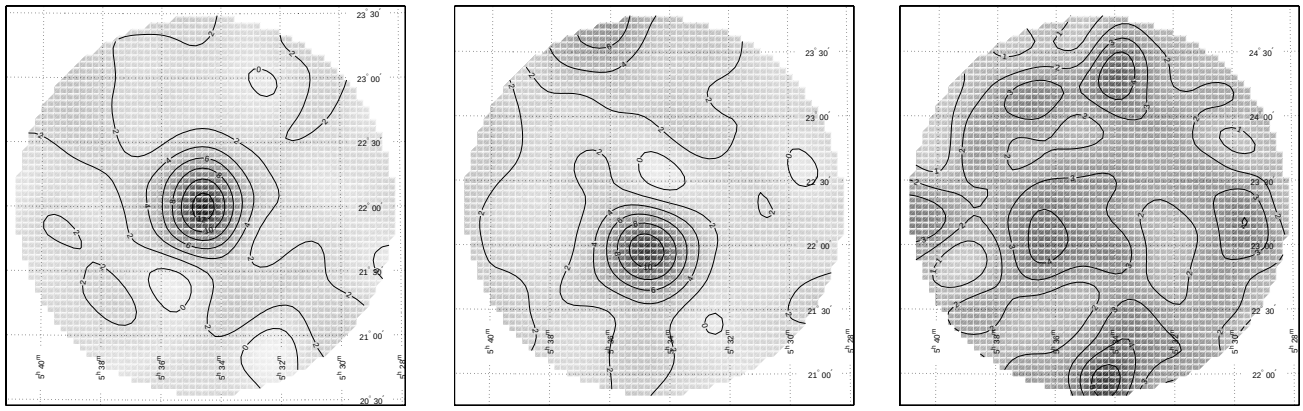

FIG. 3.—Observations of the Crab Nebula, offset by varying amounts from the center of the field of view. The contours show detection significance. The observations at an offset of 1.°3 place the Crab outside the geometrical field of view.

clearly visible. At an offset of 0.°3 the γ-ray collection efficiency is 84% of its on-axis value. At an offset of 1.°3, with the source outside of the geometrical extent of the camera, the efficiency is 30%. The significance map for these data show appreciable background contamination over the field due to the simple reconstruction approach of assigning the arrival direction of each photon to two points on the shower axis. More sophisticated approaches can reduce such false sources (Lessard et al. 2001).

In this analysis, a map of (a priori) significance is produced and the EGRET 95% contour level overlaid. The area of the region inside the contour is used to calculate an equivalent number of independent bins. This value is then used to calculate a significance level that is equivalent to the accepted Gaussian 4 σ confidence level. The map is checked for emission from within the region of interest.

6. RESULTS

The results of the observations are summarized in Table 4, which gives the upper limits (at the 99% confidence level) for a source anywhere within the EGRET 95% confidence region. Where identifications have been suggested, the upper limit for the candidate is presented in Table 5. Figure 4 presents maps of upper limit contours from the VHE observations with the EGRET confidence contours superposed. The spectral measurements from the EGRET observations, from the online version of the 3EG catalog (Hartman et al. 1999), are shown in Figure 5 together with an extrapolation of the power-law spectrum to TeV energies and the upper limits from Table 4. Spectral energy distributions (SEDs) for a selection of sources, from archival data, are presented in Figure 6. Significance maps for excess TeV γ-ray–like events from the Whipple observation of the two unidentified sources 3EG J1337+5029 and 3EG J2227+6122 are shown in Figures 7 and 8, respectively.

6.1. *3EG J0010+7309*

The 3EG source J0010+7309 has been associated with the SNR CTA 1, G119.5+10.2 in Green (2001), on the basis of its position. X-ray observations indicate that emission from CTA 1 must be described by three components; the first is a thermal, shell-type component associated with the Sedov expansion of the remnant into the interstellar medium (ISM), producing a large shell-type nebula $\sim$107′ in diameter and 1.4 $\pm$ 0.3 kpc in distance. There is a ''blowout'' region to the north where the nebula has evidently expanded quickly into a region of particularly low density. The second X-ray component is associated with a region of bright, nonthermal emission at the center of the nebula. This emission is consistent with synchrotron emission from a central nebula, with a differential power-law spectral index of 2.3 and total X-ray luminosity of $L_{\rm X} = 5.6 \times 10^{33}$ ergs s^{-1}. Finally, *ROSAT* detected a nonthermal compact point source, RX J0007.0+7302, which may be associated with a pulsar at the center of the nebula, although no pulsations have been detected in radio or X-rays. Slane et al. (2004) report on *XMM* observations of the compact source; its spectrum is best fitted by a power law with a differential spectral index of 1.5 and total luminosity of $L_{\rm X} = 4.7 \times 10^{31}$ ergs s^{-1}.

Brazier et al. (1998) suggest that the 100 MeV γ-rays from this source are most likely associated with the compact source, which lies within the 95% confidence contour of the EGRET observations. The power-law X-ray spectrum of the compact source can be extrapolated to γ-ray energies without a spectral break. Brazier et al. (1998) noted a possible cutoff in the highest energy part of the EGRET spectrum that would support a pulsar origin, although the statistics are not compelling. Other compact X-ray sources in the region are suggested as possible counterparts by Seward et al. (1995); Brazier et al. (1998) dismiss all but RX J0010+7309.

Figure 5*a* shows the EGRET power-law spectrum extrapolated to 350 GeV, with the upper limit superposed. A cutoff in the spectrum is required to reconcile these observations. Some evidence for this cutoff is also visible in the highest energy bins of the EGRET spectrum. The cutoff supports the supposition that the γ-rays originate from a pulsar. The upper limit on the integral flux from the point-source RX J0007.0+7302 is $F(>350\ {\rm GeV}) < 1.1 \times 10^{-11}$ cm^{-2} s^{-1}.

6.2. *3EG J0241+6103*

First detected by the *COS B* instrument, and designated as 2CG 135+01, the strong γ-ray source 3EG J0241+6103 has been the subject of much study over the past 25 years. Observations with EGRET refined the position estimate leaving the nonthermal radio source GT 0236+610 (Gregory & Taylor 1978; Hermsen et al. 1977) as the most likely candidate. The nonthermal radio source is associated with the binary system LSI +61°303 (Gregory et al. 1979), an unusual object that has been identified at radio, optical, and X-ray energies. LSI +61°303 exhibits radio outbursts at a period of $\sim$26.5 days (Taylor & Gregory 1982). There is evidence that both the phase and amplitude of the outbursts vary slowly with a $\sim$4.6 yr phase modulation period (Gregory et al. 1999; Gregory 2002). Paredes et al.

TABLE 4
Upper Limits for Unidentified EGRET Fields

Source Name	Coordinates α (J2000.0)	Coordinates δ (J2000.0)	Extent (deg × deg)	Upper Limit (10^{-11} cm^{-2} s^{-1})
3EG J0010+7309	00 09 36.6	+73 10 57.4	0.25 × 0.22	2.2
3EG J0241+6103	02 41 31.3	+61 04 12.3	0.21 × 0.15	2.2
3EG J0423+1707	04 23 56.5	+16 56 27.4	0.88 × 0.65	6.6
3EG J0433+2908	04 33 35.1	+29 07 42.2	0.19 × 0.16	1.6
3EG J0450+1105	22 15 06.5	+31 28 55.7	0.65 × 0.61	5.0
3EG J0613+4201	06 14 20.6	+41 59 51	0.66 × 0.46	4.3
3EG J0628+1847	06 28 36.1	+18 50 35	0.66 × 0.49	4.1
3EG J0634+0521	06 34 39.9	+05 28 21	0.85 × 0.50	5.3
3EG J0631+0642	06 31 39.4	+06 41 42	0.55 × 0.39	6.0
GeV J0633+0645	06 33 08.8	+06 45 49	0.42 × 0.42	4.9
3EG J1009+4855	10 09 59.3	+48 50 30	1.12 × 0.80	4.6
3EG J1323+2200	13 23 20.1	+22 02 52	0.52 × 0.43	3.1
3EG J1337+5029	13 38 00.8	+50 25 57	0.77 × 0.66	5.9
3EG J1826−1302	18 26 01.0	−13 05 28	0.55 × 0.39	4.2
3EG J1823−1314	18 23 24.7	−13 14 32	0.33 × 0.23	3.2
GeV J1825−1310	18 25 14.3	−13 10 19	0.32 × 0.32	4.2
3EG J1835+5918	18 35 24.9	+59 19 15.3	0.16 × 0.13	3.8
GeV J1907+0557	19 07 40.4	+05 57 14	0.38 × 0.28	3.0
GeV J2020+3658	20 20 45.1	+36 58 50	0.28 × 0.21	3.7
3EG J2021+3716	20 21 19.9	+37 15 12	0.35 × 0.26	3.7
3EG J2016+3657	20 16 34.1	+36 52 22	0.68 × 0.44	5.8
3EG J2227+6122	22 27 20.8	+61 23 28.9	0.50 × 0.41	4.1
GeV J2227+6101	22 27 45.9	+61 01 22.7	0.54 × 0.54	3.5
3EG J2248+1745	22 48 54.3	+17 47 09.5	1.13 × 0.78	5.2

Notes.—Coordinates are given for the center of an ellipse fitted to the EGRET 95% confidence contour, from Mattox et al. (2001) or Lamb & Macomb (1997), as appropriate. Units of right ascension are hours, minutes, and seconds, and units of declination are degrees, arcminutes, and arcseconds. The upper limit on the integral γ-ray flux above an energy of 350 GeV is at the 99% confidence level.

(1997) report a periodic modulation of the X-ray light curve from the All Sky Monitor instrument on the *RXTE* X-ray satellite, which appears to occur at a constant orbital phase, corresponding to the periastron. No pulsations have been detected in the X-ray signal, suggesting that the X-ray emission is not directly from a neutron star companion. Massi et al. (2001) report the existence of a one-sided radio jet from the object on a milliarcsecond scale. A number of models have been suggested to explain the radio and X-ray emission and to account for the possibility of γ-ray emission. Gregory & Neish (2002) provide an introduction to the observational status of this object.

Figure 4*b* shows a map of upper limits of emission from the region with the location of LSI +61°303 and QSO 4U0241+61 indicated with a cross (near the center and displaced by 1° to the north, respectively). It is evident from the figure that the binary system lies outside of the 95% confidence contour of the EGRET data, although it does lie within the considerably larger 95% confidence circle from the GeV catalog. There are no good X-ray candidates within the 95% EGRET confidence contour for this source.

LSI +61°303 was previously observed with the Whipple Telescope between 1996 and 1999, with no significant excess of γ-rays being detected; an integral flux limit of $F(>500\ \mathrm{GeV}) < 0.88 \times 10^{-11}$ cm^{-2} s^{-1} was reported by Hall et al. (2003). Assuming that the 3EG source corresponds to the LSI +61°303, Hall et al. (2003) show that an cutoff is required in the extrapolated EGRET spectrum to accommodate the VHE observations (lighter arrow at 500 GeV depicted in Fig. 5*b*). Most of the allowed possible range for the extrapolated flux at 350 GeV is ruled out by the upper limit reported here. After a quarter century of study, 2CG 135+01 remains one of the most puzzling of all γ-ray sources.

6.3. *3EG J0423+1707*

3EG J0423+1707 is an EGRET source about which very little is known at other wavelengths. The 3EG error circle is large, at $0.^{\circ}88 \times 0.^{\circ}65$, and the source has the softest spectrum of all of the sources chosen for this survey. Mattox et al. (2001) suggest that the radio source B0422+1749 as a possible, but unlikely, counterpart, with a probability of 2×10^{-4}. Sowards-Emmerd et al. (2003) list a plausible flat-spectrum radio quasar (FSRQ) counterpart at redshift of $z = 0.91$, too distant to be detectable by Whipple at 350 GeV owing to absorption of the γ-ray signal with the intergalactic infrared radiation field (IIRF; see, e.g., Vassiliev 2000). As is clear from Figure 5*c*, the VHE limit does not constrain the extrapolated EGRET spectrum.

6.4. *GeV J0433+2907*

The EGRET source J0433+2908 is listed as possibly being associated with the radio source 87GB 0430+2859, assumed to be an AGN. The identification is sufficiently certain that this source should probably not now be considered as "unidentified" (Foreman et al. 2001; Sowards-Emmerd et al. 2003). The source is unusual for an EGRET AGN; the spectrum is particularly hard, with no indication of a break at energies up to 10 GeV. Dingus & Bertsch (2001) analyzed all of the EGRET photons at

TABLE 5

Upper Limits for Candidates in Unidentified EGRET Fields

Source Name	Coordinates		Extent	Upper Limit
	α (J2000.0)	δ (J2000.0)	(deg × deg)	(10^{-11} cm^{-2} s^{-1})
3EG J0010+7309:				
RX J0007.0+7302	00 07 02.2	+73 03 07.1	...	1.1
3EG J0241+6103:				
LSI +61 303	02 40 31.4	+61 13 45.6	...	1.7
QSO 4U0241+61	02 44 37.3	+62 13 57.0	...	2.3
3EG J0423+1707:				
B0422+1749	04 24 53.4	+17 55 49.9	...	2.8
3EG J0433+2908:				
87GB 0430+2859	04 33 37.5	+29 05 53.0	...	0.8
3EG J0450+1105:				
B0446+1116	04 49 07.7	+11 21 28.6	...	1.3
GeV J0508+0540:				
RX J0509.3+0541	05 09 26.0	+05 41 35.4	...	0.73
3EG J0613+4201:				
87GB 0609+4123	06 12 51.2	+41 22 37	...	1.9
87GB 0612+4131	06 16 22.4	+41 30 48	...	3.1
87GB 0614+4209	06 18 08.6	+41 08 00	...	2.9
3EG J0628+1847:				
87GB 0624+1833	06 27 20.5	+18 31 04	...	1.5
87GB 0628+1911	06 31 32.3	+19 08 41	...	2.6
3EG J0634+0521:				
SAX J0635+0533	06 35 17.4	+05 33 21	...	2.0
Mon OB 2A	06 32 10.2	+04 50 46	0.33 × 0.47	4.7
HD46150	06 30 36.0	+04 57 00	...	3.1
HD46223	06 31 00.0	+04 50 00	...	2.4
3EG J1009+4855:				
87GB 1011+4941	10 15 04.1	+49 26 01	...	3.3
3EG J1323+2200:				
87GB 1324+2226	13 27 00.8	+22 10 50	...	2.1
87GB 1318+2231	13 21 11.2	+22 16 12	...	2.1
87GB 1319+2203	13 22 11.4	+21 48 12	...	1.6
87GB 1321+2229	13 24 14.9	+22 13 08	...	1.2
3EG J1337+5029:				
A1758	13 32 31.7	+50 30 41	0.18 × 0.18	6.9
87GB 1329+5023	13 31 37.2	+50 07 55	...	3.6
87GB 1340+5125	13 42 23.5	+51 10 18	...	3.9
J133510.2+503920[a]	13 35 10.2	+50 39 20	...	3.5
RX J1335.3+5015	13 35 19.6	+50 15 04	...	3.0
RX J1337.3+5032	13 37 20.0	+50 32 52	...	2.5
J134023.3+503113[a]	13 40 23.3	+50 31 13	...	2.1
J134350.8+503016[a]	13 43 50.8	+50 30 16	...	3.0
3EG J1826−1302:				
PSR B1823−13	18 26 13.2	−13 34 47	...	2.4
SNR 18.1−0.2	18 24 37.0	−13 15 18	0.03 × 0.01	2.6
AX J1826.1−1300	18 26 04.9	−12 59 48	...	3.7
G16.8−1.1	18 25 20.0	−14 46 00	0.25 × 0.25	6.9
G18.8−0.3 (Kes 67)	18 23 58.0	−12 23 00	0.14 × 0.14	6.8
G18.9−1.1	18 29 50.0	−12 58 00	0.28 × 0.28	3.6
Sct OB 3	18 25 27.2	−14 15 04	1.30 × 1.00	6.2
J183015.9−140807[a]	18 30 15.9	−14 08 07	...	4.6
J182920.6...130914[a]	18 29 20.6	−13 09 14	...	2.0
3EG J1835+5918:				
RX J1836.2+5925	18 36 13.7	+59 25 30.1	...	3.7
GeV J1907+0557:				
AX J1907.1+0549	19 07 21.3	+05 49 14	...	2.6
G39.2−0.3	19 03 58.7	+05 26 19	0.07 × 0.07	3.6
G40.5−0.5	19 07 05.6	+06 30 06	0.18 × 0.18	4.0
G41.1−0.3	19 07 29.4	+07 07 35	0.04 × 0.04	6.3

TABLE 5—*Continued*

Source Name	Coordinates α (J2000.0)	Coordinates δ (J2000.0)	Extent (deg × deg)	Upper Limit (10^{-11} cm^{-2} s^{-1})
GeV J2020+3658:				
PSR J2021+3651	20 21 07.8	+36 51 19	...	2.0
TXS B2013+370	20 15 28.4	+37 11 02	...	2.0
G74.9+1.2	20 15 40.3	+37 11 52	0.07 × 0.07	2.1
WR 137	20 14 32.7	+36 39 46	...	5.5
WR 138	20 17 00.4	+37 25 24	...	2.0
WR 141	20 21 33.2	+36 55 36	...	2.1
WR 142	20 21 38.2	+37 23 38	...	1.9
3EG J2227+6122:				
PSR J2229+6144	22 29 05.3	+61 14 09.3	...	2.2
87GB B2226+6122	22 28 38.0	+61 37 42.0	...	2.8
3EG J2248+1745:				
A2486	22 48 45.0	+17 09 30.0	...	1.7
3EG J2255+1943:				
J225617.9+205257[a]	22 56 17.9	+20 52 57.0	...	4.4
J225906.4+192637[a]	22 59 06.4	+19 26 37.0	...	2.7

Notes.—Units of right ascension are hours, minutes, and seconds, and units of declination are degrees, arcminutes, and arcseconds. The upper limit on the integral γ-ray flux above an energy of 350 GeV is at the 99% confidence level.

[a] The standard RASS-BSC prefix of 1RXS is omitted for formatting purposes.

energies above 10 GeV and showed that three photons are consistent with having originated from the location of the radio source, with a probability of 1.9×10^{-6} of the correlation occurring by chance.

Assuming that the γ-ray source indeed corresponds to the radio/X-ray source, an SED for 3EG J0433+2908 based on archival data is shown in Figure 6. No successful redshift measurements have been made for this object, Halpern et al. (2003) report on repeated attempts to determine the redshift and argue that $z > 0.3$.

The upper limit on VHE emission is displayed with the 3EG spectrum in Figure 5*d*. To reconcile the limit with the increasing EGRET spectrum a cutoff in the spectrum at an energy greater than 10 GeV is required. For this candidate, additional observations were made pointed directly at the radio/X-ray source. These data provide a more sensitive limit on emission from the point source. An integral flux limit of $F(>350\ \mathrm{GeV}) < 0.76 \times 10^{-11}\ \mathrm{cm}^{-2}\ \mathrm{s}^{-1}$ is derived from all of these data combined, and is displayed in Figure 6. It must be noted that the figure was produced with *non-contemporaneous* data and should be considered as approximate. The double-peaked structure is clearly visible, with the peak in the synchrotron emission occurring somewhere in the optical to X-ray band and the peak in the IC emission occurring between the high-energy and VHE γ-ray regimes.

It is reasonable to conclude that there is a cutoff between 10 and $\sim$100 GeV, either due to a feature intrinsic to the source spectrum or due to absorption of the γ-ray signal in the IIRF (considering $z > 0.3$). Alternatively, it is possible that the state of the object was different when the various observations were made, i.e., flaring when EGRET observed it and quiescent during the VHE observations, in which case a cutoff may not be required. However, since the EGRET spectrum is calculated as a mean over all viewing periods, it is unlikely to correspond purely to the source spectrum during flaring periods.

6.5. *3EG J0450+1105*

3EG J0450+1105 has one of the softer spectra of the sources chosen in this survey but is listed as a "source of GeV gamma rays based upon the search for repeating, weak outbursts" in the second part of the GeV catalog (Macomb & Lamb 1999) and is consistent with being variable at 100 MeV.

Mattox et al. (2001) suggest that the γ-ray source is associated with the radio source B0446+1116, an AGN. Halpern et al. (2003) confirm this association and present their attempts to resolve a redshift for the object. They claim that the accepted redshift of $z = 1.207$ is likely incorrect, and that the featureless spectrum they obtained makes it impossible to derive an unambiguous redshift. Depending on how the minor features in the spectrum are interpreted, they suggest $z = 0.74$ or $z = 0.21$ as possible values for the redshift, with the lower value being less likely. Figure 6 shows the SED for the radio source obtained from published data. The SED shows the two-peaked structure typical of a low-frequency peaked BL Lac (LBL). The upper limit derived for the location of the radio source is also shown. Because of the soft spectrum, the VHE upper limit does not constrain the emission significantly.

6.6. *GeV J0508+0540*

GeV J0508+0540 is listed in the GeV catalog as a "low-significance source" and was not detected significantly at 100 MeV. Dingus & Bertsch (2001) list two EGRET photons with energies greater than 40 GeV consistent with coming from the object. On the basis of the improved PSF at these energies, the photons are attributed to the BL Lac 0509+056, with high probability. Halpern et al. (2003) report several unsuccessful attempts to measure the redshift of this object; the optical spectra they recorded were featureless and no host galaxy could be resolved.

Assuming that the association with the BL Lac is correct, this source was observed in the "Tracking" mode, which is optimized for point-source objects. No emission map is presented in Figure 4, the limit at 350 GeV is shown in Figure 5*e*.

6.7. *3EG J0613+4201*

3EG J0613+4201 is a 100 MeV and 1 GeV γ-ray source at mid-Galactic latitude with a relatively hard spectrum, weak flux, and large error box. Although Nolan et al. (2003) list a relatively

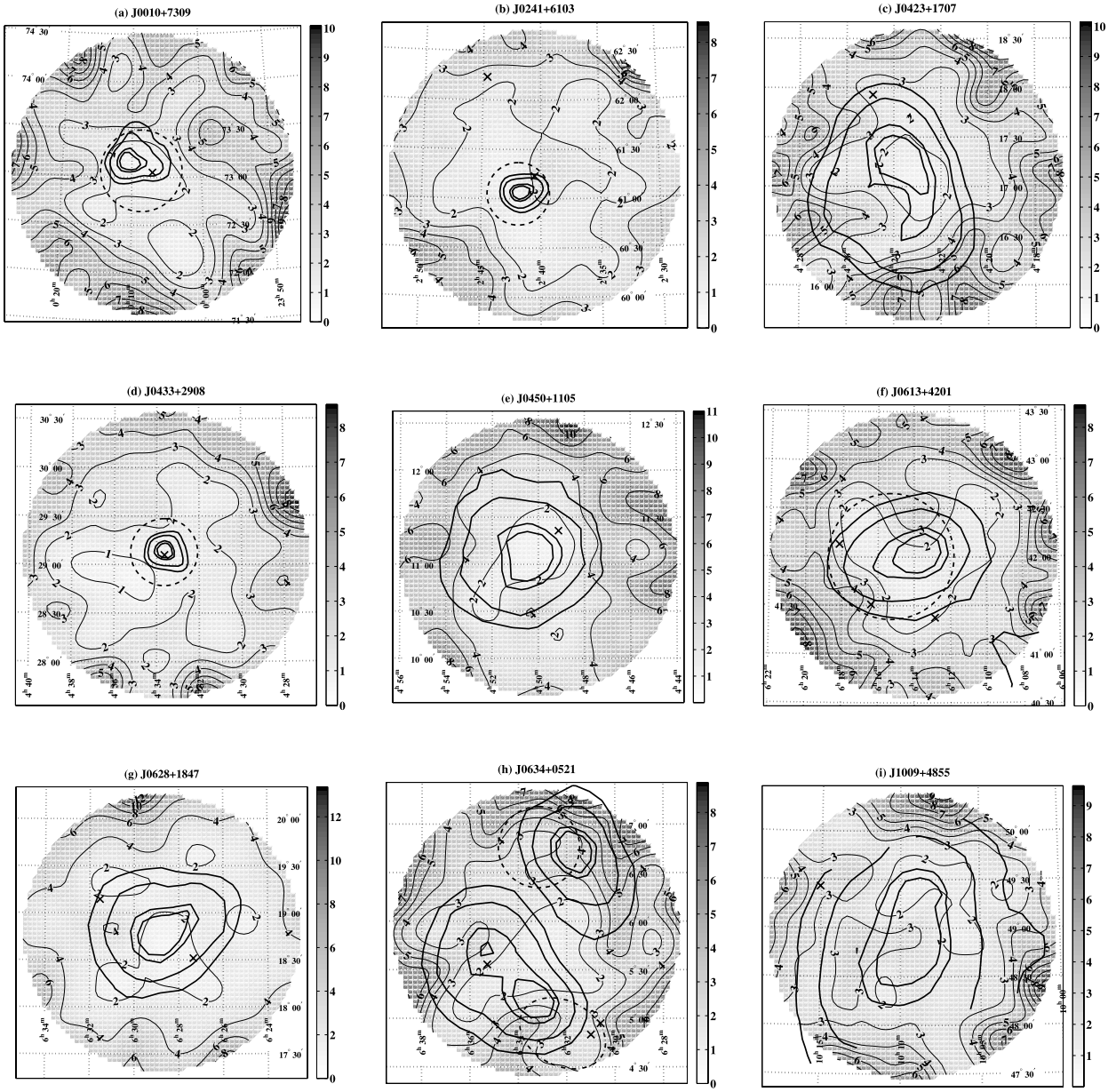

FIG. 4.—Upper limits on emission in units of 10^{-11} cm^{-2} s^{-1}.

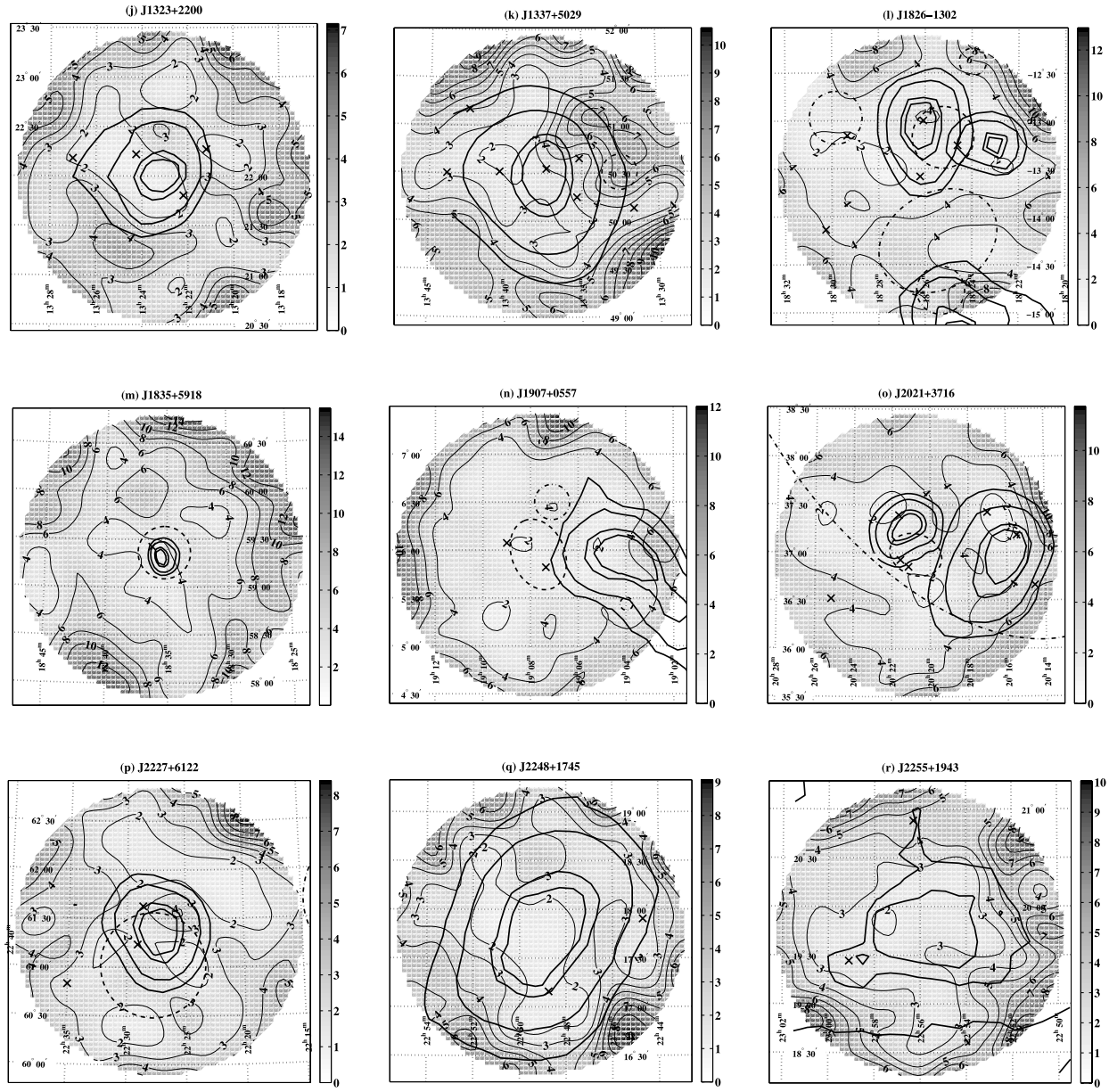

FIG. 4.—*Continued*

large variability index, the 68% lower bound on the index is consistent with a steady source. Mattox et al. (2001) list three possible radio counterparts for the source, all outside of the 95% 3EG contour. None of the potential associations are very compelling, in each case the probability of the association being correct is listed as $\leq 10^{-4}$. The limit calculated from our observations is not sensitive enough to rule out a simple extrapolation of the EGRET spectrum into the VHE regime.

6.8. *3EG J0628+1847*

Despite being close to the Galactic plane, Romero et al. (1999) report no positional associations for 3EG J0628+1847 with known SNRs, OB associations, or W-R and O-type stars. Mattox et al. (2001) list two radio sources from the Green Bank catalog in the field, one just inside the 95% confidence contour, the other just inside the 99% contour. The second, 87GB 0628+1971, is coincident with a *ROSAT* X-ray source (Laurent-Muehleisen et al. 1997) and has an associated IR point source in the Two Micron All Sky Survey catalog.

The VHE upper limit for the full EGRET field does not constrain an extrapolation of the EGRET spectrum to 350 GeV (Fig. 5*g*). Assuming that the γ-ray source is associated with 87GB 0628+1911, an approximate SED for the object is shown in Figure 6. The VHE limit appropriate to the source location does not significantly constrain the spectrum above 10 GeV.

6.9. *3EG J0634+0521 and 3EG J0631+0642*

The γ-ray sources 3EG J0634+0521 and 3EG J0631+0642 both lie in the region of the Monoceros SNR, although neither is explicitly associated with it in the 3EG catalog. In addition, the source GeV J0633+0645 partially overlaps 3EG J0631+0642 and is listed as a possible counterpart to the SNR in Lamb & Macomb (1997).

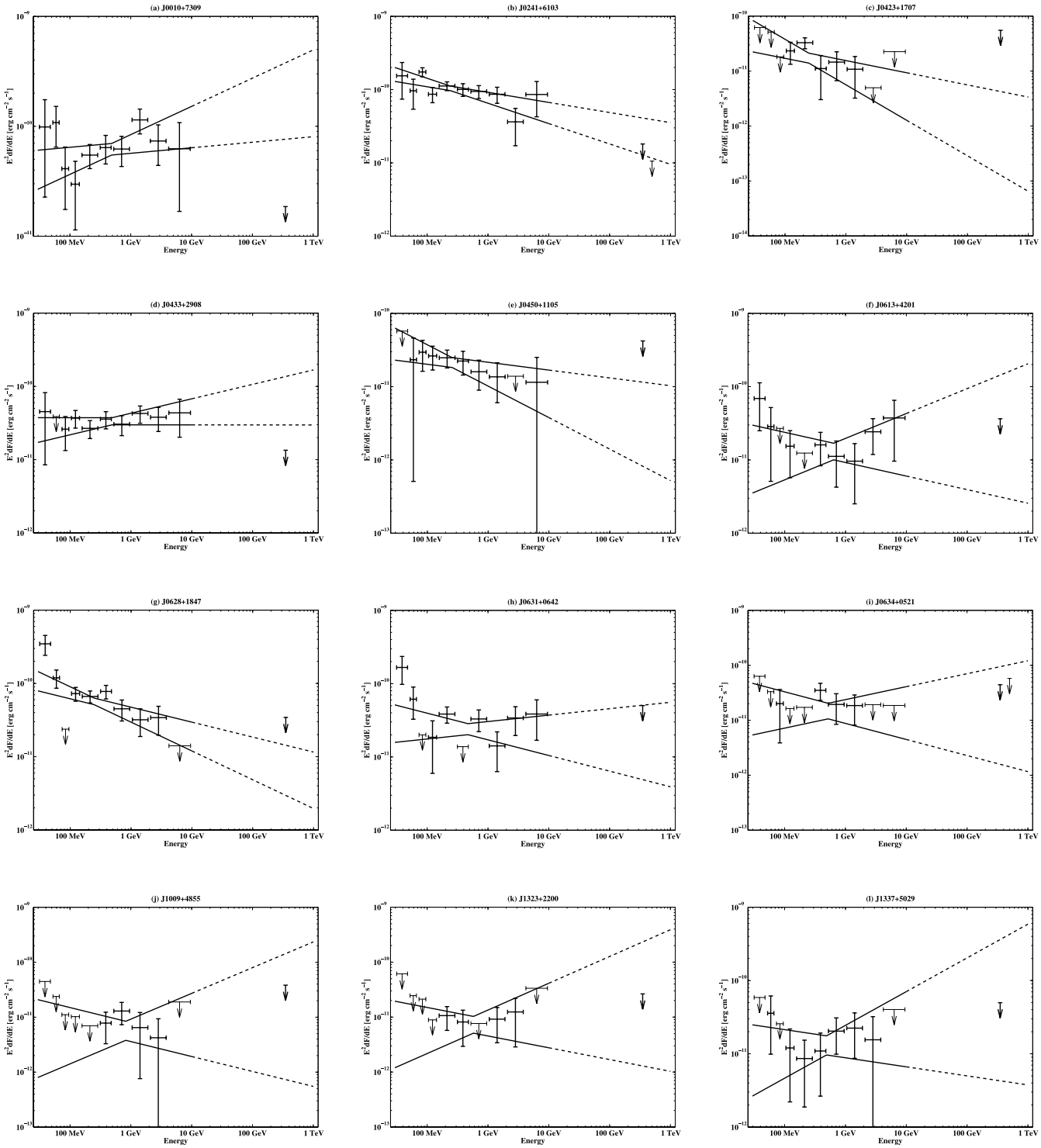

FIG. 5.—Spectra from the 3EG catalog with the upper limits at 350 GeV (*heavy arrows*) from observations with the Whipple 10 m telescope as presented in Table 4. In the cases of 3EG J0241+6103 and 3EG J0634+0521, previous limits at 500 GeV from Hall et al. (2003) and Lessard et al. (1999), respectively, are shown as lighter arrows. In the cases of 3EG J2016+3657 and 3EG J2021+3716 the limits for the most likely associations are indicated, as described in the text. [*See the electronic edition of the Journal for a color version of this figure*.]

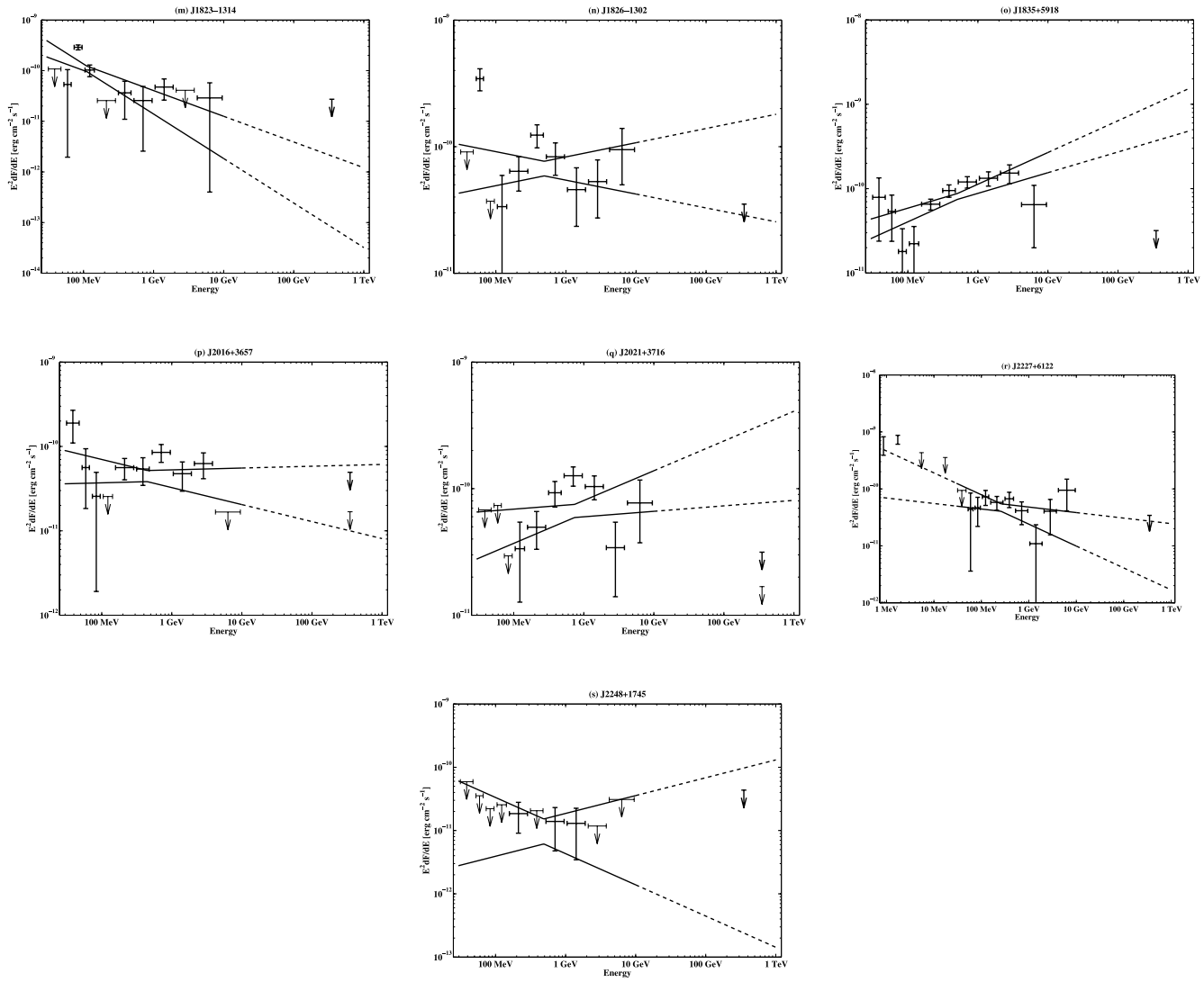

FIG. 5.—*Continued*

The shell-type SNR G205.5+0.5, or Monoceros Loop Nebula, is 220′ in diameter, the fifth largest SNR in Green (2001). The SNR is thought to be 1.39 ± 0.1 kpc distant and approximately $(3-20) \times 10^4$ yr in age, i.e., in the Sedov expansion phase. Monoceros was first recognized as a source of 100 MeV γ-rays by Esposito et al. (1996). Jaffe et al. (1997) presented a map of EGRET γ-ray emission over a large area around the SNR, in which they found evidence for an extended emission feature in the direction of the Rosette nebula. They suggest that, since γ-ray emission was not seen uniformly across the remnant, the γ-rays are produced in a region of enhanced shock acceleration at the interaction between the remnant and the nebula. Kaaret et al. (1999) used the *BeppoSAX* narrow-field instruments to image the region around 3EG J0634+0521 and discovered a point source with a hard spectrum, SAX J0635+0553. They report an optical counterpart, which is likely a B-type companion star, and conclude that if the γ-ray emission is associated with the system (or a portion of it is), then it is a γ-ray–emitting X-ray binary. Further X-ray observations revealed a 33.8 ms pulsation (Kaaret et al. 2000). In a recent study of all potential EGRET SNR counterparts, Torres et al. (2003) suggest that the source of the γ-ray emission is far from resolved. The fact that *BeppoSAX* did not discover extended emission from the region, as would be expected in a shock acceleration scenario, suggests that the binary may be responsible for the γ-ray emission. However, no orbital variations are seen in the γ-ray signal. Analysis of the pulsar energetics and accretion rate further confuses the issue; see Torres et al. (2003) for a review. Lucarelli et al. (2001) report preliminary evidence for VHE γ-ray emission from the region with the HEGRA telescope system. The VHE emission was extended and was not coincident with the *BeppoSAX* source. No measurement was given.

Torres et al. (2003) suggest that 3EG J0634+0521 might be a composite source, with the *BeppoSAX* source being responsible for a portion of the EGRET γ-ray flux and the bulk of the X-ray emission, while interactions between the SNR and the Rosette Nebula may contribute to the 3EG flux and account for any VHE emission. They predict that if a composite source is responsible, a spectral break should be detected between the EGRET and ground-based γ-ray regimes. For 3EG J0631+0642 a pure shock acceleration model is sufficient to explain the 3EG flux.

Romero et al. (1999) studied potential positional associations between 3EG sources and SNRs, OB associations, and W-R type and O-type stars. They report two O-type stars and two OB associations in the region in addition to the Monoceros SNR: from a catalog of O-type stars (Cruz-González et al.

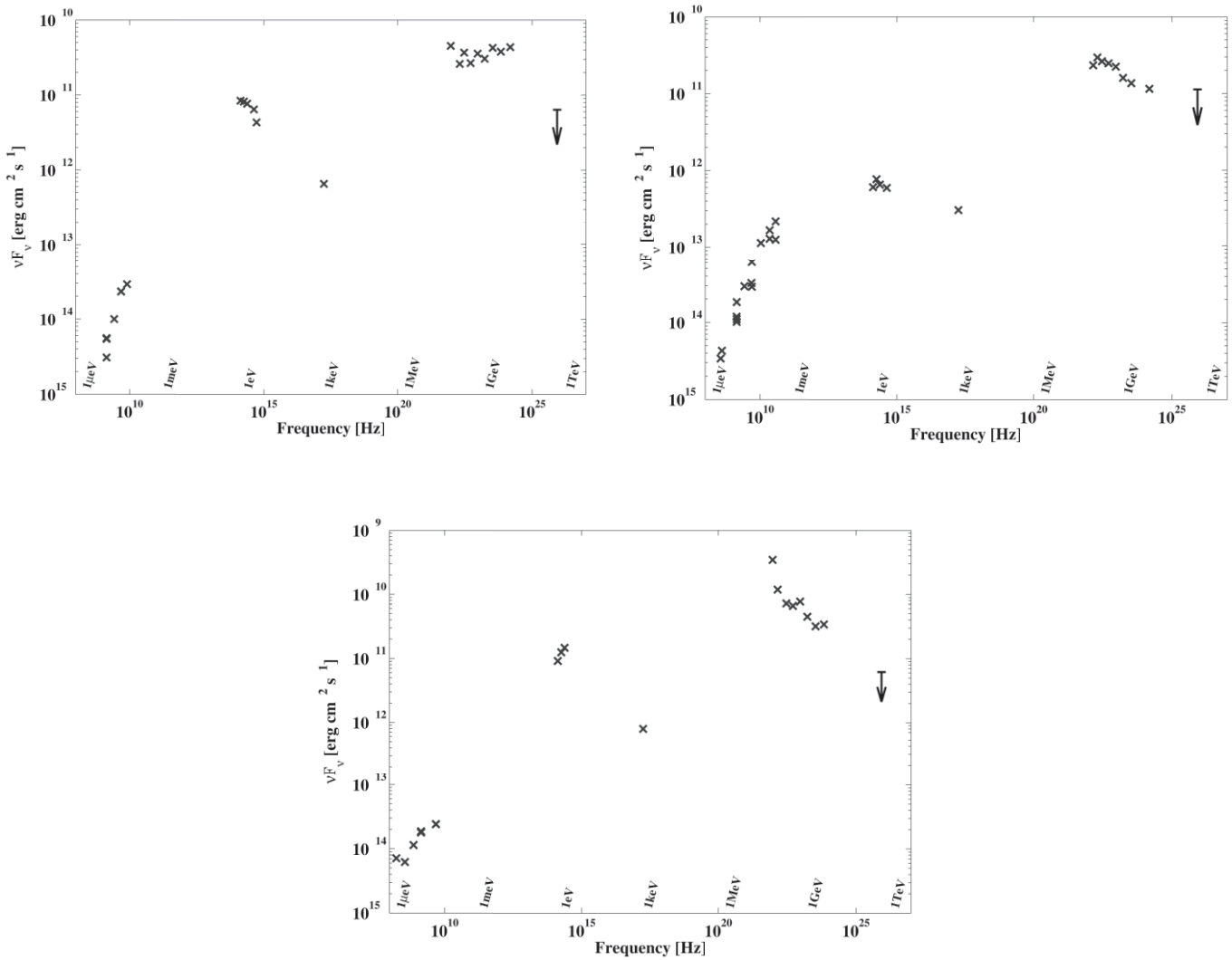

FIG. 6.—Spectral energy distribution (SED) for 3EG J0433+2907 (*top left*), 3EG J0450+1105 (*top right*), and GeV J0628+1847 (*bottom*) from noncontemporaneous, archival data. The upper limits at 350 GeV from observations with the Whipple 10 m telescope as presented in Table 5 are shown as heavy arrows. [*See the electronic edition of the Journal for a color version of this figure.*]

1974) HD 46150 and HD 46223 and from a catalog of OB-associations (Mel'Nik & Efremov 1995) Mon OB 2A and Mon OB 1B.[25] Mon OB 1B lies just outside of the region studied in this work.

No significant VHE emission was detected in the field; Figure 4*h* presents the upper limits derived from the observations. The figure shows the EGRET contours for both sources, with 3EG J0634+0521 toward the lower left. The GeV source is indicated as a dashed circle overlapping 3EG J0631+0642. The dash-dotted circle toward the bottom of the figure indicates the location of Mon OB 2A, with the two O-type stars, each marked by a cross within. Finally, the location of SAX J0635+0533 is marked as a cross near the center of 3EG J0634+0521.

The extrapolated EGRET spectra for both sources are shown in Figures 5*h* and 5*i* with the upper limits at 350 GeV. These observations do not require a break in the spectrum of either source and cannot substantiate (or refute) the two-component model of Torres et al. (2003). Although the previous upper limits derived from observations with the Whipple Telescope (Lessard et al. 1999) had a lower flux value, the observations were made at higher energy and do not constrain the extrapolated EGRET spectrum. The previous limits are shown on the figure at 500 GeV.

6.10. *3EG J1009+4855*

Very little is known about 3EG J1009+4855 at other wavelengths. The EGRET catalog suggests a weak association with the radio/X-ray source B1011+496, a known AGN at redshift of $z = 0.2$. Mattox et al. (2001) list the probability of that association as 2×10^{-4}; the radio source lies outside of the large 99% error contour, and the association seems unlikely. The VHE upper limit does not significantly constrain the wide range of flux uncertainties in the 3EG spectrum.

6.11. *3EG J1323+2200*

EGRET detected variable emission from the high-latitude source 3EG J1323+2200. During most of the viewing periods (VPs) for which it was in the field of view no emission was detected; during VP 308.0 a flux of $(68.4 \pm 22.6) \times 10^{-8}$ cm^{-2} s^{-1} was measured, more than 10 times the time-averaged flux listed in the catalog. The source is listed in the GeV catalog as

[25] Romero et al. (1999) refer to Mon OB 2B, which is not in the catalog. Mon OB 1B is the correct source association.

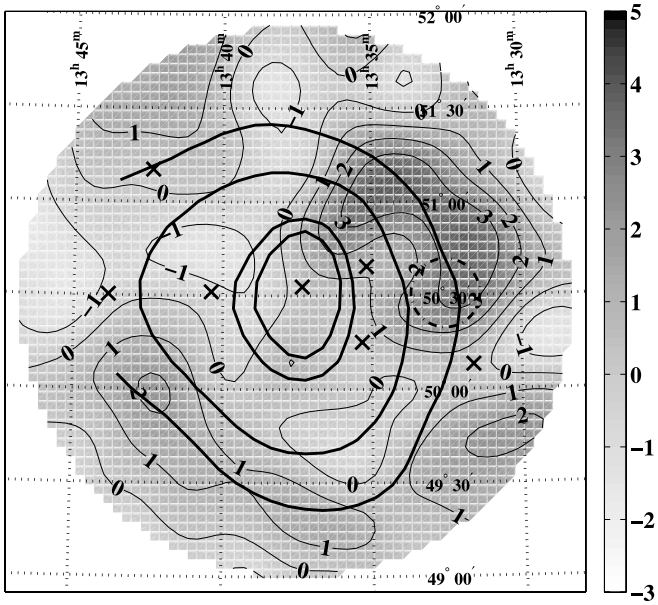

FIG. 7.—Significance of excess γ-ray–like events detected from the region of 3EG J1337+5029 (*light solid lines*). The 3EG likelihood contours are shown as heavy lines, the cluster is shown as a dot-dashed circle, and the various other sources in the field are shown as crosses.

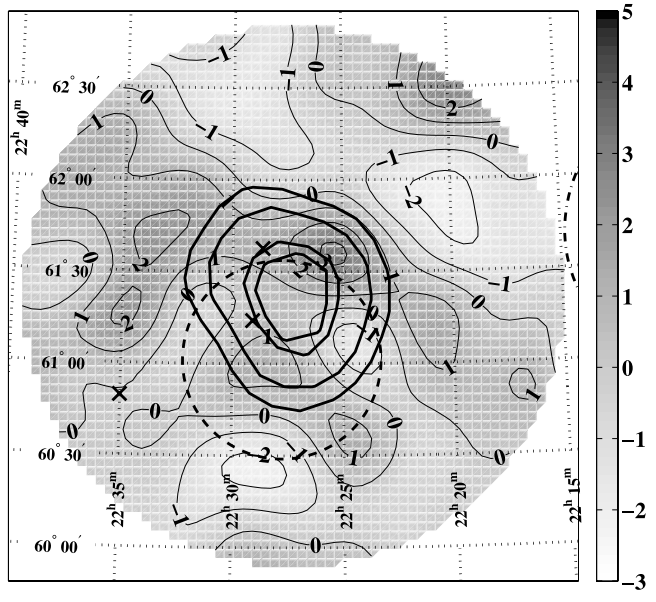

FIG. 8.—Significance of excess γ-ray–like events, detected from the region of 3EG J2227+6122 (*light solid lines*). The 3EG likelihood contours are shown as heavy lines. The GeV source location is indicated by the heavy dashed line and the nearby OB association as a dot-dashed line which barely overlaps the region, to the west.

a "source of GeV gamma rays based upon a search for repeating, weak outbursts." Mattox et al. (2001) lists four potential associations with radio sources, two of which are within the 95% confidence contour. The most likely association, just outside of the 95% contour, is listed as having a probability of ~1%. Sowards-Emmerd et al. (2003) list three candidates with redshifts of $z > 0.9$, none of which are regarded as having "high confidence." Upper limits on emission are presented in Figure 4*j* with the four radio sources, displayed as crosses. The limits do not significantly constrain an extrapolation of the EGRET spectrum to 350 GeV.

6.12. *3EG J1337+5029*

The γ-ray source 3EG J1337+5029, at Galactic latitude of +65°, has a spectral index of 1.83 ± 0.29, the fourth hardest among the unidentified sources. Nolan et al. (2003) list the variability as being consistent with a steady source at the 68% confidence level; it was detected significantly in four of six VPs.

Colafrancesco (2002) suggests that the γ-ray source is associated with the galaxy cluster A1758 (Abell et al. 1989), with diameter 22′ and redshift $z = 0.279$. However, a subsequent reanalysis of the coincidence between EGRET sources and known clusters (Reimer et al. 2003) has ruled out this association. Indeed, the association with the cluster is cast into doubt when the EGRET confidence contours are plotted; the cluster lies outside of the 95% probability contour to the west.

Four radio sources from the NRAO VLA Sky Survey (NVSS) are coincident with the cluster. There are five additional *ROSAT* All-Sky Survey Bright Source Catalog (RASS-BSC) X-ray sources in the field, four within the 95% contour; some have radio counterparts in the NVSS. The RASS-BSC lists some potential associations for the X-ray sources, two with stars, and one with an AGN and a star. Limits are presented for each of the X-ray sources irrespective of these associations. Mattox et al. (2001) list two unlikely radio associations from the Green Bank catalog, one outside of the 99% contour, the other just inside. These seven sources are shown on Figure 7. Two X-ray sources inside the cluster have been omitted in light of the combined, extended source discussed by Böhringer et al. (2000).

The VHE observations result in a broad excess, approximately $1.^{\circ}0 \times 0.^{\circ}5$ in extent, which lies along the 99% contour to the northwest of the 3EG catalog position. The significance of the excess is plotted in Figure 7. The peak in the excess has an a priori statistical significance of ~4 σ, making it the most significant of all the observations in this survey. Since emission was not predicted from this particular location a priori, the true probability of obtaining such a result by chance, given the number of sources observed in this survey and the combined size of the EGRET error boxes must be evaluated. This is done by first calculating the number of "independent measurements" in the survey. For example, it is estimated that ~200 measurements lie within the 95% contours for the 18 sources analyzed using the two-dimensional technique in this survey. An equivalent Gaussian significance of the probability of obtaining such a result by chance can then be calculated. In the case of a 4 σ excess with 200 trials, the equivalent significance is ~2.5 σ. Since this excess is not within the 95% contour, but rather the 99% contour, the number of trials is larger than 200 and its true significance lower than ~2.5 σ. Given this conservative approach and that the data set for this source is so small (~2.5 hr), we do not claim to have seen emission from this source. However, the excess gives an a priori expectation of emission from this location, and is a strong reason to make follow-up observations.

Since VHE emission is not claimed, upper limits for the region and potential associations are presented in Figure 4*k*. Figure 5*l* shows the upper limit, which rules out half of the flux space allowed by extrapolating the EGRET spectrum to 350 GeV. Ongoing observations will either detect emission from this source or further constrain its spectrum.

6.13. *3EG J1826−1302 and 3EG J1823−1314*

The low-latitude γ-ray sources 3EG J1826−1302 and 3EG J1823−1314 are close enough that they both lie in the Whipple

camera field of view. 3EG J1826−1302 has a relatively hard, well-determined spectrum and a large 100 MeV flux, and shows evidence of being variable, while 3EG J1823−1314 has a softer spectrum, a large flux, and is less variable. The centers of the sources lie approximately $0.^{\circ}8$ apart, a separation that is considerably smaller than the EGRET point-spread function at 100 MeV; they are listed in the 3EG catalog as having positions, fluxes, and significances that could be affected by source confusion. GeV J1825−1310 overlaps both of the 3EG sources but is more consistent with 3EG J1826−1302. A third EGRET source, 3EG J1824-1514, is also close to these sources ($\sim 2^{\circ}$) and is partially within the field of view of the VHE observations, as described below.

ASCA observations of the region (Roberts et al. 2001) reveal a previously unknown extended X-ray source, denoted AX J1826.1−1300, thought to be a pulsar wind nebula (PWN). The putative PWN is centered on the source 3EG J1826−1302 and makes a good potential counterpart for the γ-ray source. A pulsar/PWN origin would account for the hardness of the EGRET spectrum. The variability index of $\delta = 0.88$ is indicative of a variable source and consistent with the mean value for the known PWN γ-ray sources (Nolan et al. 2003), but inconsistent with the mean value for pulsars. The *ASCA* images show extended emission near the nonthermal radio source SNR 18.1−0.2, reported as a possible SNR by Odegard (1986), but not adopted as such by Green (2001). This emission is consistent with the 100 MeV source 3EG J1823−1314.

The much studied PSR B1823−13, a young, energetic, Vela-like pulsar, is contained within the 95% error contour of 3EG J1826−1302. The source has been targeted for VHE observations with the Whipple (Hall et al. 2001 and references therein) and HEGRA (Aharonian et al. 2002; identified as PSR J1826−1334) telescopes, with integral flux limits of $F(>520\ \mathrm{GeV}) < 0.91 \times 10^{-11}\ \mathrm{cm}^{-2}\ \mathrm{s}^{-1}$ and $F(>1700\ \mathrm{GeV}) < 0.48 \times 10^{-11}\ \mathrm{cm}^{-2}\ \mathrm{s}^{-1}$ being derived, respectively. Gaensler et al. (2003) present deep *XMM-Newton* observations of the pulsar, in which they discover two components of emission, a core of hard X-ray emission of $5''$ extent surrounded by an asymmetric region of fainter, softer, diffuse emission toward the south of the pulsar. They do not detect the radio pulsar, either as a compact point source or through pulsations. No associated SNR is seen.

Green (2001) report three SNRs within the field of view of the VHE observations, one of which, G18.8−0.3 (or Kes 67), was suggested by Sturner & Dermer (1995) as a candidate for a source in the first EGRET catalog (GRO 1923−12 from Fichtel et al. 1994). None of the SNRs (shown as the three smaller dot-dashed ellipses in Fig. 4*l*) are within the 95% confidence contours of the two EGRET sources reported on here. Romero et al. (1999) lists a positional coincidence between the three EGRET sources in the field and the OB association Sct OB 3. The association (largest dot-dashed ellipses in Fig. 4*l*) does not significantly overlap 3EG J1826−1302 or 3EG J1823−1314 but does show some overlap with 3EG J1826−1302 and with the SNR G16.8−11. Previous VHE limits for the three SNRs (and for many other Galactic SNRs) have been presented by the HEGRA collaboration (Aharonian et al. 2002). Mattox et al. (2001) do not have potential radio candidates for these 3EG sources. The RASS-BSC contains two X-ray sources in the field.

The VHE upper limits for both objects are displayed in Figures 5*m* and 5*n*. The limit derived for the region of 3EG J1826−1302 constrains the hard EGRET spectrum to the softest spectrum allowed by the errors in the 100 MeV flux and spectral index. It is likely that a cutoff in the spectrum occurs between the highest EGRET flux point, at 6 GeV, and the VHE observations. In the case of 3EG J1823−1314, the softer EGRET spectrum is not constrained by the VHE upper limit.

6.14. *3EG J1835+5918*

3EG J1835+5918 has the hardest spectral index and smallest error circle among all the EGRET sources classified as unidentified. The source was detected consistently throughout the EGRET mission. The hard spectrum and low variability suggest an association with a pulsar, although none have been definitively identified in the field.

The source has been extensively studied at radio, optical, and X-ray energies by two independent groups (see Reimer et al. 2002; Halpern et al. 2002 and references therein), who present compelling evidence that the source is associated with an isolated neutron star, possibly a radio-quiet, Geminga-like pulsar. Mirabal et al. (2000) report on a series of observations with many different instruments across the spectrum, which narrowed the list of potential *ROSAT* and *ASCA* X-ray candidate associations in the 95% error contour from 10 to 1: RX J1836.2+5925. Optical/UV photometry uncovered 40 possible AGNs in the field, based on a search for broad UV continuum emission. Twenty radio sources were found in archival VLA observations or standard radio catalogs. No flat-spectrum radio sources, which could correspond to FSRQs and BL Lacs, the only AGN identified as EGRET sources to date, were identified in the field. Follow-up optical spectra of the candidates revealed that most of the X-ray sources were distant AGN or G- to M-type stars. Only RX J1836.2+5925, the brightest of the *ROSAT* sources, was unidentified in the initial optical survey, and it was selected as the mostly likely counterpart for the γ-ray source, although its properties were unlike any other known EGRET source.

Mirabal & Halpern (2001) report a reanalysis of the *ROSAT* data in which soft X-ray emission below 0.4 keV became apparent, which they conclude is thermal emission from the surface of an isolated neutron star. Subsequent observations with the *Chandra* X-ray satellite and *Hubble Space Telescope* (*HST*; Halpern et al. 2002) make this conclusion very compelling; the excellent resolution of the *Chandra* instrument rules out all possible optical counterparts in the *HST* image, down to the limiting magnitude of $V > 28.5$. These observations make an association with an AGN very unlikely and constrain the distance and temperature of a neutron star (NS) candidate. They conclude that it must be very distant (compared with the Geminga pulsar), with $d \approx 800$ pc. Given a standard model for NS cooling, they calculate an age of $\sim 10^6$ yr. No SNR was detected around the pulsar in sensitive VLA observations; it seems likely that the NS was ejected from the remnant at birth and traveled to its present location. If the NS started in (or near) the Galactic plane and the putative distance of 800 pc is correct, the NS must have traveled a distance of 340 pc to reach its present location (latitude of $b = 25^{\circ}$); Halpern et al. (2002) conclude that such a distance is not unreasonable, given the age of the NS.

The limit on the VHE emission, displayed in Figure 5*o*, constrains an extrapolation of the EGRET spectrum. A cutoff is required in the spectrum between the highest EGRET energies and 350 GeV, supporting the case for a pulsar origin of the γ-rays. Reimer et al. (2001) and Halpern et al. (2002) suggest independently that this cutoff is visible in the 4 GeV EGRET point, which is considerably below the expected power-law flux.

6.15. *GeV J1907+0557*

The GeV source J1907+0557 does not have a counterpart 100 MeV EGRET source, although 3EG J1903+0550 is listed incorrectly in the 3EG catalog as being associated with it; there

is very little overlap at the 95% confidence level. Sturner & Dermer (1995) suggest that a first EGRET catalog source in the region is associated with the SNR G40.5−0.5; an association of the SNR with the revised positions of the GeV and 3EG sources seems unlikely. There are two additional SNRs in the region listed by Green (2001), but neither is a likely counterpart for the GeV source. One of them (G39.2−0.3) is listed by Torres et al. (2003) as a counterpart to the 3EG source. Roberts et al. (2001) present an *ASCA* image of the GeV source in which they have discovered an extended X-ray source, AX J1907.4+0557. No other X-ray sources appear in the *ASCA* image, which covers approximately half of the region within the GeV 95% contour.

The center of the GeV source was observed with the Whipple instrument. These observations show a large excess of γ-ray–like events whose reconstructed origins are distributed across the on-source region, from the center of the field to a distance of $>1\overset{\circ}{.}8$ from the center, by which point the number of events drops quickly because of the limited field of view of the instrument. It is unlikely that such a broad excess is the result of γ-ray emission from a large, extended source; rather it is likely to be the result of a difference in brightness between the on- and off-source regions that is not completely compensated for by the data analysis algorithm. In order to remove this systematic effect, the number of events in an annulus defined by $1\overset{\circ}{.}4 <$ dist $< 1\overset{\circ}{.}8$ (Reynolds et al. 1993) is calculated from the on-source and off-source data and their ratio is used to scale the number of off-source counts to the number in the on-source region. After this rescaling, no significant excess or deficit is present. An upper limit to the integral flux of $F(>350\ \mathrm{GeV}) < 3.0 \times 10^{-11}\ \mathrm{cm}^{-2}\ \mathrm{s}^{-1}$ is placed on emission from within the GeV error circle. The HEGRA group derive a limit on the integral flux of $F(>700\ \mathrm{GeV}) < 0.3 \times 10^{-12}\ \mathrm{cm}^{-2}\ \mathrm{s}^{-1}$ from this source based on a considerably longer exposure (Rowell et al. 2003).

6.16. *GeV J2020+3658 (3EG J2021+3716 and 3EG J2016+3657)*

The first two catalogs of EGRET point sources listed a γ-ray source in the region of the field of the *COS B* source 2CG 075+00. Further data resolved two separate sources, 3EG J2021+3716 and 3EG J2016+3657, each with a differential spectral index of $\sim$2.0. The GeV catalog also lists a source in the region, GeV J2020+3658, which is suggested in the 3EG catalog as a counterpart for 3EG J2016+3657. Roberts et al. (2001) note that the GeV source is more likely to be associated with 3EG J2021+3716, with which it has considerable overlap.

An *ASCA* image of the GeV source region revealed two bright X-ray sources, one corresponding to a massive W-R binary star system (WR 141) with a 21.6 day periodicity (Roberts et al. 2001). The second, identified as AX J2021.1+3651 was seen to have a nonthermal spectrum; subsequent investigations with the Arecibo radiotelescope revealed a young, energetic pulsar, PSR J2021+3651, with period of 104 ms (Roberts et al. 2002). The *ASCA* image also reveals extended X-ray emission, which may be thermal emission from an SNR or a nearby massive star. The pulsar is an intriguing candidate for the γ-ray source, in light of its hard spectrum and relatively low variability. The pulsar is located well within the 95% confidence region of the GeV source. Its positional association with the 3EG source is less clear; it lies just outside of the 99% contour. If the 3EG and GeV sources correspond to the same object, the W-R star system is a better positional association, although it is not contained within the 95% contour of the 3EG source. Finally, a second W-R type star, WR 142, is located north of the 3EG catalog position, well within the 95% region. Source confusion between the adjacent EGRET sources probably means that there are systematic errors in the positions of the confidence contours for both 3EG sources and the GeV source. Roberts et al. (2002) conclude that the pulsar is the most conservative association, being a member of the only class of Galactic γ-ray sources to be unambiguously identified to date.

Mukherjee et al. (2000) and Halpern et al. (2001a) present detailed multiwavelength observations of 19 X-ray sources from the *ROSAT* faint source catalog consistent with 3EG J2016+3657. Most have stellar associations: W-R type systems, binaries, cataclysmic variables, and O- and B-type stars that are members of the OB association Cyg OB 1. These candidates are generally dismissed by Halpern et al. (2001a). Two *ROSAT* sources appear to be plausible candidates for the γ-ray emission, one an SNR G74.9+1.2 (or CTB 87), the other a flat spectrum radio source TXS B2013+370 (or G74.87+1.22), which overlaps the position of the SNR but is not related to it. The SNR has a filled center morphology, flat radio spectrum, and high polarization, typical of a synchrotron nebula. No associated pulsar has been detected. Based on its low X-ray luminosity and large distance of 12 kpc, Halpern et al. (2001a) argue that the energetics of the system are not sufficient to account for the γ-ray source. Multiwavelength observations of TXS B2013+370 (Mukherjee et al. 2000) reveal that it has the properties of a blazar at radio, optical, and X-ray wavelengths. The flux variability seen in the EGRET data was also seen in optical observations of the radio source. Halpern et al. (2001a) conclude that, based on the population of 66 well-identified blazars at higher Galactic latitudes, it would be expected to find at least one in the region of $-1^\circ < b < +1^\circ$. A redshift is not known for this object.

Romero et al. (1999) suggest that the γ-ray emission may be associated with the OB association listed as Cyg OB 1 ,8, 9 in the catalog of Mel'Nik & Efremov (1995). The OB association is large ($\sim 6\overset{\circ}{.}5 \times 3\overset{\circ}{.}5$) and is listed as a possible counterpart to six EGRET sources, including the two of concern here. Finally, the RASS-BSC lists two bright X-ray sources. One corresponds to WR 138; the other is located far from the EGRET sources but is displayed in Figure 4*o* for completeness.

In the case of 3EG J2021+3716, the VHE observations constrain an extrapolation of its hard spectrum, Figure 5*q*. If the association with the pulsar is correct, the upper limit for the pulsar constrains the emission further, as indicated in the figure by the lighter shaded upper limit at 350 GeV. A cutoff in the spectrum above 10 GeV is required to accommodate either limit; such a cutoff is consistent with the hypothesis that the object is associated with a pulsar. In the case of 3EG J2016+3657, Figure 5*p*, the emission is not well constrained by the limit for the large 3EG error box, which extends close to the edge of the field of view of the VHE observations, where the instrument is significantly less sensitive. If the blazar or SNR association is correct, the emission is somewhat constrained by the limit, although not significantly (lighter upper limit in Fig. 5*p*).

6.17. *3EG J2227+6122*

Halpern et al. (2001b, 2001c) report on multiwavelength observations of six possible X-ray counterparts in the region of 3EG J2227+6122. Optical observations identified five of the sources with stars; the sixth remained unidentified. Radio observations revealed only one radio source, coincident with the unidentified X-ray source, which was subsequently identified as a young, 51.6 ms radio pulsar: PSR J2229+6144. Since the radio and γ-ray observations were not contemporaneous, and the timing ephemeris for a young pulsar cannot be extrapolated back in time as the pulsations are unstable, a search for pulsations in

the EGRET data could not be performed. Halpern et al. (2001c) conclude that since no other X-ray or radio counterpart is found to be consistent with the γ-ray source, it is more conservative to accept the association with the pulsar than to reject it.

Mattox et al. (2001) noted that 87GB B2226+6122, a radio source that corresponds to a Galactic H II region (Sharpness 141), lies within the error box. In addition, Romero et al. (1999) list the OB association Cep OB 2B as a possible counterpart, although there is no overlap between the 95% contour of the 3EG source and the OB association; their centers are separated by $\sim 3\overset{\circ}{.}8$.

VHE observations result in an excess of γ-ray–like events within the 95% confidence contour, at an a priori significance of 3.2 σ (Fig. 8). The excess does not coincide with the pulsar or with the only RASS-BSC X-ray source in the region (1RXS J223500.5+604935). Given that there is no a priori reason to expect emission from the location of the excess, the post-trial probability of obtaining such an excess is calculated to have an equivalent Gaussian significance of $\sim$1.2 σ. As in the case of 3EG J1337+5029, the probability is below what is required to claim a detection. The upper limit does not significantly constrain the extrapolated EGRET spectrum (Fig. 5*r*).

6.18. *3EG J2248+1745*

Very little is known about this source. Colafrancesco (2002) note that the cluster A2248, at redshift of $z = 0.143$, lies within the 95% contour, but it is an unlikely counterpart owing to the variability of the EGRET source. Mattox et al. (2001) list the well-studied flat-spectrum radio source 87GB B2251+1552 (3C 454.3, an AGN at $z = 0.86$) as an unlikely association. The radio source lies well outside of the 99% contour and is a far more likely counterpart for 3EG J2254+1601. The RASS-BSC contains one bright X-ray source with the EGRET 99% contour, 1RXS J224441.6+175418. Because of the large uncertainty in the EGRET location, the VHE upper limit for the source region is higher than most of the limits presented in this survey. An extrapolation of the EGRET spectrum to 350 GeV is not significantly constrained by the limits.

6.19. *3EG J2255+1943*

The EGRET source 3EG J2255+1943 has the largest positional error and variability index of all of the sources considered in this survey. The diameter of the 95% error contour is larger than the field of view of the Whipple camera, and the contour is not closed in the significance map from the online version of the 3EG catalog. Since the total error box is not contained within the field of view of the instrument, an upper limit is not presented for the source.

7. DISCUSSION

Multiwavelength observations have proved to be the most powerful tool available to investigate the origin of the high-energy emission from the unidentified EGRET sources. For a number of such sources, X-ray, radio, and optical observations have narrowed the list of scientifically viable, potential candidates. In some cases, such observations have ruled out all but one candidate. This survey was undertaken in the hope that VHE emission would be detected from one of the sources chosen and that the higher spatial resolution achievable with the ground-based technique would allow the source of the γ-ray emission to be identified. There is significant overlap between the VHE source catalog (Horan & Weekes 2004) and the EGRET sources; seven of the 18 credible VHE sources were also seen by EGRET at some level. Of the two categories of sources unambiguously identified by EGRET, blazars and pulsars, detections of eight BL Lac type blazars have been claimed at TeV energies. No pulsars have been directly detected by ground-based instruments, but some EGRET pulsars are associated with PWN which, like the Crab may be visible to VHE γ-ray instruments.

In total, results from VHE observations of 21 EGRET sources are reported, more than 10% of the unidentified source population. The observations yielded an average of 5 hr of data from each source. When the survey was initiated, little was known about many of the observed sources, outside of what was published in the 3EG catalog. Since that time, our understanding of these sources has advanced considerably, both through work on the population as a whole and through multiwavelength observations of individual sources. Of particular note in the first category is the calculation of source variability by Nolan et al. (2003) and the systematic correlation of the sources with radio sources (Mattox et al. 2001) and SNRs, OB associations, and massive stars (Romero et al. 1999). Through multiwavelength studies, six of the sources studied here can now be considered identified: 3EG J0010+7309 (possible pulsar), 3EG J0241+ 6103 (variable radio source), 3EG J0433+2907 (blazar at $z > 0.3$), 3EG J1835+5918 (neutron star), GeV J2020+3658 (radio pulsar), and 3EG J2227+6122 (radio/X-ray pulsar). None of these would have been considered a good candidate for TeV emission.

Some of the fainter, mid-latitude EGRET sources could be accounted for by Geminga-like pulsars. In fact, several of the recent suggested identifications for the low-latitude EGRET sources have turned out to be pulsars. Pulsar models predict cutoffs below 350 GeV; hence it is not surprising that none were detected in this survey. Polar-cap models predict a sharper cutoff and a smaller population of radio-quiet pulsars than the outer-gap models (Harding et al. 2004; Zhang et al. 2000). If there is a large population of radio-quiet γ-ray pulsars resulting from outer-gap emission, they may be detectable with the next generation of ground-based γ-ray instruments such as VERITAS and HESS.

Based on the number of observations made (i.e., the number of sources surveyed and the number of independent bins in each two-dimensional image), it cannot be claimed that VHE γ-ray emission was detected from any of the sources at a significant level. Two of these sources, 3EG J1337+5029 and 3EG J2227+6122, have excesses with sufficiently low chance probability that they would be considered as suggestive of γ-ray emission if the observations were taken in isolation from the rest of the survey. In the case of J1337+5029, the location of the VHE excess corresponds to the location of a cluster, A1758. If the excess is the result of γ-ray emission from the cluster, it would represent a new class of VHE emission and it would be the most distant source of VHE emission to date (at $z = 0.279$, considerably more distant than H1426+428, the most distant VHE blazar, at $z = 0.129$) and have important implications for the density of the IIRF. The location of the VHE excess in the case of J2227+6122 does not correspond to any of the suggested associations for the EGRET source. To confirm (or refute) any emission, independent follow-up observations will be made. The excesses correspond to fluxes of 0.40 and 0.33 times the integral Crab Nebula flux, at energies >350 GeV, respectively. At this level, a 5–10 hr exposure on each source will be sufficient for confirmation.

The next generation of ground-based instruments are more than an order of magnitude more sensitive than the Whipple 10 m telescope (Fig. 1). They are most sensitive to γ-rays at approximately $\sim$100 GeV, with some sensitivity even below this energy. A survey of EGRET sources with one of these instruments should have considerable success in detecting γ-ray emission.

We acknowledge the technical assistance of K. Harris, E. Roache, J. Melnick, and E. Little. This research is supported by grants from the US Department of Energy, the National Science Foundation, Science Foundation Ireland, and P.P.A.R.C. in the U.K. S. Fegan acknowledges the support of the Predoctoral Fellowship program at the Smithsonian Astrophysical Observatory. We gratefully acknowledge the useful suggestions made by the anonymous referee.

REFERENCES

Abell, G. O., Corwin, H. G., & Olowin, R. P. 1989, ApJS, 70, 1
Aharonian, F. A., et al. 2002, A&A, 395, 803
Akerlof, C. W., et al. 1991, ApJ, 377, L97
Böhringer, H., et al. 2000, ApJS, 129, 435
Brazier, K. T. S., Reimer, O., Kanbach, G., & Carramiñana, A. 1998, MNRAS, 295, 819
Buckley, J. H., et al. 1997, in Proc. 25th Int. Cosmic Ray Conf. (Durban), 3, 233
Cawley, F. M., et al. 1990, in Proc. 21st Int. Cosmic Ray Conf. (Adelaide) 4, 224
Colafrancesco, S. 2002, A&A, 396, 31
Cruz-González, C., et al. 1974, Rev. Mex. AA, 1, 211
Dingus, B. L., & Bertsch, D. L. 2001, in AIP Conf. Proc. 587, Gamma 2001, Gamma-Ray Astrophysics, ed. S. Ritz, N. Gehrels, & C. Shrader (Melville: AIP), 251
Esposito, J. A., Hunter, S. D., Kanbach, G., & Sreekumar, P. 1996, ApJ, 461, 820
Fegan, S. J., et al. 2001, in AIP Conf. Proc. 587, Gamma 2001, Gamma-Ray Astrophysics, ed. S. Ritz, N. Gehrels, & C. Shrader (Melville: AIP), 296
Fichtel, C. E., et al. 1994, ApJS, 94, 551
Finley, J. P., et al. 1999, in AIP Conf. Proc. 515 GeV–TeV Gamma Ray Astrophysics Workshop, ed. B. Dingus, M. Salamon, & D. Kieda (Melville: AIP), 301
Foreman, J., et al. 2001, BAAS, 33, 1453
Gaensler, B. M., et al. 2003, ApJ, 588, 441
Gehrels, N., Macomb, D. J., Bertsch, D. L., Thompson, D. J., & Hartman, R. C. 2000, Nature, 404, 363
Green, D. A. 2001, A Catalogue of Galactic Supernova Remnants (Cambridge: Mullard Radio Astron. Obs.)
Gregory, P. C. 2002, ApJ, 575, 427
Gregory, P. C., & Neish, C. 2002, ApJ, 580, 1133
Gregory, P. C., Peracaula, M., & Taylor, Gregory, P. C. 1999, ApJ, 520, 376
Gregory, P. C., & Taylor, A. R. 1978, Nature, 272, 704
Gregory, P. C., et al. 1979, AJ, 84, 1030
Hall, T. A., et al. 2001, in Proc. 27th Int. Cosmic Ray Conf. (Hamburg), 2485
———. 2003, ApJ, 583, 853
Halpern, J. P., Eracleous, M., & Mattox, J. R. 2003, AJ, 125, 572
Halpern, J. P., Eracleous, M., Mukherjee, R., & Gotthelf, E. V. 2001a, ApJ, 551, 1016
Halpern, J. P. Gotthelf, E. V., Leighly, K. M., & Helfand, D. J. 2001b, ApJ, 547, 323
Halpern, J. P., Gotthelf, E. V., Mirabal, N., & Camilo, F. 2002, ApJ, 573, L41
Halpern, J. P., et al. 2001c, ApJ, 552, L125
Harding, A. K., et al. 2004, Adv. Space Res. 33, 571
Hartman, R. C., et al. 1999, ApJS, 123, 79
Hermsen, W., et al. 1997, Nature, 269, 494
Holder, J., et al. 2003, ApJ, 583, L9
Horan, D., & Weekes, T. C. 2004, NewA Rev., 48, 527
Horan, D., et al. 2002, ApJ, 571, 753
Jaffe, T. R., Bhattacharya, D., Dixon, D., D. & Zych, A. D. 1997, ApJ, 484, L129
Kaaret, P., Cusumano, G., & Sacco, B. 2000, ApJ, 542, L41
Kaaret, P., Piraino, S., Halpern, J., & Eracleous, M. 1999, ApJ, 523, 197
Kosack, K., et al. 2004, ApJ, 608, L97
Krennrich, F., et al. 2002, ApJ, 575, L9
Lamb, R. C., & Macomb, D. J. 1997, ApJ, 488, 872
Laurent-Muehleisen, S. A., et al. 1997, A&AS, 122, 235
Lessard, R. W., Buckley, J. H., Connaughton, V., & Le Bohec, S. 2001, Astropart. Phys., 15, 1
Lessard, R. W., et al. 1999, in Proc. 26th Int. Cosmic Ray Conf. (Salt Lake City), 488
Lucarelli, F., et al. 2001, in AIP Conf. Proc. 558, High Energy Gamma-Ray Astronomy, ed. F. A. Aharonian & H. Volk (Melville: AIP), 779
Macomb, D. J., & Lamb, R. C. 1999, in Proc. 26th Int. Cosmic Ray Conf. (Salt Lake City), 107
Massi, M., et al. 2001, A&A, 376, 217
Mattox, J. R., Hartman, R. C., & Reimer, O. 2001, ApJS, 135, 155
Mel'Nik, A. M., & Efremov, Y. N. 1995, Astron. Let., 21, 10
Mirabal, N., & Halpern, J. P. 2001, ApJ, 547, L137
Mirabal, N., Halpern, J. P., Eracleous, M., & Becker, R. H. 2000, ApJ, 541, 180
Mukherjee, R., Gotthelf, E. V., Halpern, J., & Tavani, M. 2000, ApJ, 542, 740
Nolan, P. L., et al. 2003, ApJ, 597, 615
Odegard, N. 1986, AJ, 92, 1372
Paredes, J. M., Marti, J., Peracaula, M., & Ribo, M. 1997, A&A, 320, L25
Punch, M., et al. 1992, Nature, 358, 477
Reimer, O., Pohl, M., Sreekumar, P., & Mattox, J. R. 2003, ApJ, 588, 155
Reimer, O., et al. 2001, MNRAS, 324, 772
———. 2002, in Neutron Stars, Pulsars, and Supernova Remnants, ed. W. Becker, H. Lesch, & J. Trümper (Garching: MPE), 100
Reynolds, P. T., et al. 1993, ApJ, 404, 206
Roberts, M. S. E., Romani, R. W., & Kawai, N. 2001, ApJS, 133, 451
Roberts, M. S. E., et al. 2002, ApJ, 577, L19
Romero, G. E., Benaglia, P., & Torres, D. F. 1999, A&A, 348, 868
Rowell, G., et al. 2003, in Proc. 28th Int. Cosmic Ray Conf. (Tsukuba), 2329
Schroedter, M., et al. 2002, AAS/HEAD Meeting, Abst. B17.052
Seward, F. D., Schmidt, B., & Slane, P. 1995, ApJ, 453, 284
Slane, P., et al. 2004, ApJ, 601, 1045
Sowards-Emmerd, D., et al. 2003, ApJ, 590, 109
Sturner, S. J., & Dermer, C. D. 1995, A&A, 293, L17
Taylor, A. R., & Gregory, P. C. 1982, ApJ, 255, 210
Torres, D. F., et al. 2003, Phys. Rep., 382, 303
Vassiliev, V. V. 2000, Astropart. Phys., 12, 217
Zhang, L., Zhang, Y. J., & Cheng, K. S. 2000, A&A, 357, 957